ALMA MATER STUDIORUM · UNIVERSITÀ DI BOLOGNA

Scuola di Scienze
Dipartimento di Fisica e Astronomia
Corso di Laurea Magistrale in Fisica

MATHEMATICAL MODELLING OF INTEGRIN-LIKE RECEPTORS SYSTEMS

Relatore:
Prof. Daniel Remondini

Correlatore:
Prof. Bertrand Fourcade

Presentata da:
Adriano Moi

Anno Accademico 2015/2016

Abstract

In this work I have obtained exact non trivial stationary patterns in a integrin reaction-diffusion mathematical model. Integrins are essential adhesion cellular receptors found in the surface of all metazoan cells. They are regulators of cell migration and they mediate interaction between the cells and their extracellular matrix. In fact, they are critical for embryonic development, tissue repair and immune responses.
Integrins signaling is characterised by bidirectionality. As a matter of fact, these heterodimers are composed by a head which resides outside the cell, a body which is situated in the membrane layer, and a tail which lies inside the cell. This configuration permits integrins to take part in signaling in both direction, outside-in and inside-out. Recently, interest has grown in understanding integrin structure, functions and particularly their activation mechanisms. Are exactly these activation properties that motivated the introduction of the reaction-diffusion model with two states receptors under study. In the model integrins have two conformational states: activated and unactivated. As long as the integrin is in the unactivated state it can freely diffuse across the membrane, but, once activated, it is stacked in the membrane and no long diffuses. The activation of integrin in this model is caused by concentration changes of a substance, Phosphatidylinositol 4,5-bisphosphate (or PIP2), that will be called u. On the other hand, concentration changes of another subtance v will decrease activation. In the language of pattern formation u plays the role of the activator while v plays the role of the inhibitor, controlling and stopping the production of u, by binding or not to the receptors. Practically, an increase of u makes integrins change their configuration to a state with much more affinity for binding to extra cellular ligands. On the other hand, integrins can also bind reversibly to the controller protein v. When the integrin ligates with v more u is produced: in this way the inhibitor controls or regulates the

activation, with a positive feedback mechanism, very common in biology. From simple chemical reactions involving the intergrins n_l, the inhibitor v, and some inert molecule $\emptyset$ we can thereafter build a model represented by one system of differential equations activator-inhibitor and another one activated-unactivated integrins. Chemical reactions are given by:

$$n_l + v \underset{\mathrm{k}_-}{\overset{\mathrm{k}_+}{\rightleftarrows}} v \diamond n_l, \ldots \xrightarrow{1/\tau} n_l + \emptyset. \tag{1}$$

Once the equations are set, we can study the model and find a particular solution for the activator and inhibitor for a special choice of the parameters involved. Finally, we can test the model by giving as an input a region which is activated (formally that would be a step function) and see what the model predicts in terms of integrins reclutation. The results obtained follow our previsions: bound integrins are found especially on the boundaries of the activated area, whereas there are no free integrins in the activated zone.

Sommario

Nel presente lavoro, ho studiato e trovato le soluzioni esatte di un modello matematico applicato ad un sistema di recettori cellulari della famiglia delle integrine. Le integrine sono dei recettori cellulari transmembrana che si trovano su tutte le cellule di organismi complessi del regno animale. Esse sono fondamentali, in qualità di regolatori della migrazione cellulare e delle interazioni con la matrice extra-cellulare, hanno ruolo determinante in attività essenziali alla vita, quali lo sviluppo dell'embrione, la riparazione dei tessuti e le risposte immunitarie. La capacità di condurre segnali bidirezionalmente è una delle proprietà più singolari che questi eterodimeri hanno, e che risulta possibile grazie alla loro conformazione. Infatti, essi sono formati da una testa disposta esternamente alla superficie cellulare, a contatto con l'ambiente esterno, un corpo che attraversa la membrana e una doppia coda che si trova all'interno della cellula, immersa nel citoplasma. I segnali trasmessi dalle integrine dall'esterno verso l'interno della cellula ne promuovono la sopravvivenza e la proliferazione; mentre i segnali trasferiti dall'interno verso l'esterno della cellula controllano l'affinità per i ligandi extracellulari, le interazioni con la matrice, e la migrazione cellulare.
Recentemente, sono stati condotti alcuni interessanti studi riguardo alla struttura, alla funzione e ai meccanismi di attivazione di questi recettori. Sono appunto le proprietà e i meccanismi di attivazione che hanno motivato la costruzione del modello reazione-diffusione con cinetica a due livelli, di seguito preso in esame. Nel modello le integrine sono considerate come un sistema a due livelli, attivo e non attivo, come un sistema di elettroni con stato fondamentale e stato eccitato. Quando le integrine si trovano nello stato inattivo possono diffondere nella membrana, mentre quando esse si trovano nello stato attivo risultano cristallizzate nella membrana, incapaci di diffondere. L'attivazione delle integrine nel mod-

ello segue quello che in letteratura prende il nome processo di attivazione tramite PIP2. Secondo questo processo, è la variazione di concentrazione nella superficie cellulare di una sostanza chiamata attivatore (appunto il PIP2, Phosphatidylinositol 4,5-bisphosphate) che dà luogo all'attivazione delle integrine. Infatti, il contatto dell'integrina con tale sostanza attivatrice porta ad un cambiamento della conformazione della sua stessa struttura facendo così aumentare la probabilità di legame coi legandi extracellulari. Inoltre, questi eterodimeri possono legare una molecola inibitrice con funzioni di controllo e regolazione, che chiameremo v, la quale, legandosi al recettore, fa aumentare la produzione della sostanza attivatrice, che chiameremo u. In questo modo si innesca un meccanismo di retroazione positiva, molto frequente nei sitemi biologici. L'inibitore v regola il meccanismo di produzione di u, ed assume, pertanto, il ruolo di modulatore. Infatti, grazie a questo sistema di fine regolazione il meccanismo di feedback positivo è in grado di autolimitarsi. Considerando questa premessa e le caratteristiche del sistema presentato, si può costruire un modello di equazioni differenziali, partendo dalle semplici reazioni chimiche coinvolte. Le reazioni chimiche in considerazione sono:

$$n_l + v \underset{\mathrm{k_-}}{\overset{\mathrm{k_+}}{\rightleftarrows}} v \diamond n_l \ldots \xrightarrow{1/\tau} n_l + \emptyset, \tag{2}$$

Dalle reazioni si costruiscono le equazioni differenziali per le concentrazioni e, una volta che il sistema di equazioni è impostato, si possono desumere le soluzioni per le concentrazioni dell'inibitore e dell'attivatore (che sono le funzioni incognite del sistema di equazioni differenziali) per un caso particolare dei parametri. Infine, si può eseguire un test per vedere cosa predice il modello in termini di integrine. Per farlo, ho utilizzato un'attivazione del tipo funzione gradino e l'ho inserita nel sistema, valutando la dinamica dei recettori. Si ottiene in questo modo un risultato in accordo con le previsioni: le integrine legate si trovano soprattutto ai limiti della zona attivata, mentre le integrine libere vengono a mancare nella zona attivata.

Contents

List of Figures

Chapter 1

Introduction

Cells are building blocks of all known living organisms. In eukaryotic systems, cells are basically composed by a plasma membrane, cytoplasmatic material and a nucleus. The plasma membrane is a double layer of phospholipids enveloping the cytoplasm and all the different organelles while the nucleus is a membrane-enclosed organelle containing the genetic material (DNA) with biological long-term instructions. The plasma membrane constitutes the most important requirement to make life possible, being the boundary between the living cell and the extra cellular nonliving environment. However, there is not complete isolation between the cell and the exterior environment. In fact, materials outside the plasma membrane play an essential role in the life of cells. In upper multicellular organism like humans, most cells are organized in clearly defined tissues: in order to survive and work together they communicate by sending and receiving signals from the environment or from other cells. The information exchange may concern availability of nutrients, changes in temperature, or variation in light levels. Cell communication allows phenomena such as cell migration, cell growth, cell differentiation, and the three-dimensional organization of tissues and organs in embryonic development. When intercellular communication occurs, cells "talk" to each other directly and change their own internal properties in order to respond through a plenty of chemical and mechanical signals.

Cell signaling may be essentially resumed in three steps:

1. Reception
2. Transduction
3. Response

In the first stage, a signaling cell sends its message to its target through a signaling molecule. This kind of molecule binds to a specific receptor protein at the receiving cell's surface. Signals molecules include hundreds of kinds of substances, such as proteins, small peptides, amino acids, nucleotides, steroids, fatty acid derivates and even dissolved gases (e.g. nitric oxide and carbon monoxide). They can act over either short or long distances. In the short range, signals may come from contact with other cells or from the extra cellular matrix (where all the cells of the same tissue lay), whereas in the long range case it may come from other part of the organism, carried for example by blood vessels.
In this context, receptors proteins can span the cell's plasma membrane and provide specific sites for water-soluble signaling molecules to bind to. Once the molecule has been received by the target cell it triggers a series of steps in order to decode the message. Communication is only possible if a signal coming from the outside environment is able to pass the plasma membrane, producing an effect on cytoplasmatic proteins, enzymes and second messengers. The second messengers may finally reach the nucleus and transfer the signal to DNA. This kind of process is called signal transduction pathway, and it represents the overall process of converting a signal in a way that the target cell can understand and consequently respond to. Changes in DNA protein synthesis produce effects travelling in the opposite sense, from the nucleus to the cytoplasm. This may potentially occur also across the membrane up to the outside environment as a response to the incoming signal.
Response is the final stage of communication and is manifestly the result of the transduced signal. It may consist of any activity present in the tissues such as duplicating, selecting the material that enters the cell, excreting the toxic or useless waste substances etc. In order to have a response, signal molecules may either be transported across the membrane by protein-based channels, or they may directly cross the membrane (lipophilic substances). Other times, the signal does not cross the membrane by itself, but

it is transmitted by first binding to a receptor protein. Next to the linkage, the protein changes its shape and thereby passes the information to the cell. It is the latter case that will be analyzed in this work.
In this context, we are focusing on integrins, the most important family of transmembrane receptors that attach the cells to their extracellular microenvironment. Founded in all metazoan cells, integrins are specialized integral membrane proteins able to transmit information from outside the cell to the inside thanks to the capability of changing their own conformation. This change occurs when specific ligand binds to a specific docking site.
As transmembrane receptors, they pass entirely trough the lipid bilayer and thus they have domains that protrude from both the extracellular and cytoplasmatic side of the membrane. Being the main receptor proteins that cells use to bind and respond to the extracellular matrix, receptors of the integrins type are crucially important. Different environments are indeed created by laying down the extra cellular matrix (ECM) components in order to support the development of various tissues types. In this framework, integrins are found to be the major cell surface receptors used to assembly/recognize functional ECM, and to facilitate cell migration to the correct tissue location [1].
Furthermore, signals transmitted by integrins can influence differentiation, motility, growth, and even the survival of the cell. Their function makes them critical for many processes and dynamic activities essential for life such as embryonic development, tissue repair and immune responses. Embryonic development is characterized by waves of cell migration during which different cells follow different routes from one part of the embryo to another. Migrating cells are guided by proteins (e.g fibronectin), that are contained within the molecular environment through which they pass. Firstly, integrins recognize and bind extracellular fibronectin; secondly, they activate a series of intracellular processes that lead to a change in cytoskeletal conformation; eventually, the cells migrate and differentiate, each one in the right position. This is decisive to develop asymmetric organisms such humans and all the multicellular species. In the same way, integrins may lead specialized cells (leucocytes) to a wound or to a site of infection to implement immune responses. As well as in important physiologic processes, integrins are studied to describe many pathological models connected to their dysfunction. As a matter of fact, they are involved in all the main and most problematic pathologies such

as cancer and heart diseases.
Their influence in cancer is best illustrated by comparing normal and malignant cells. Most malignant cells are capable of growing while suspended in a liquid culture medium. Normal cells, in contrast, can only grow and divide if they are cultured on a solid substratum; if ordinary cells are placed in suspension cultures, they die. Regular cells are thought to die in suspension culture because their integrins are not able to interact with extracellular substrates and, as a result, are not able to transmit life-saving signals to the interior of the cell. When cells become malignant their survival no longer depends on integrins binding.
Integrins role in heart diseases, instead, it is related with platelets aggregation. Platelet aggregation is a controlled physiological process that occurs when the wall of a blood vessel is injured. It requires the interaction of a platelet-specific integrin with soluble blood proteins, such as fibrinogen and von Willebrand factor, which act as linkers that allow platelets to bind to each other and to the exposed tissue collagen stopping the hemorrhage. If occuring at an inappropriate time or place, the aggregation of platelets can form a potentially dangerous blood clot (thrombus) that can block the flow of blood to vital organs. This is one of the leading causes of heart attack and stroke. The specific interaction between integrins and their target is studied to develop drugs that could avoid inappropriate activation and prevent major cardiovascular events.

1.1 Integrins structure and working principles

There are many varieties of integrins (at least twenty four in humans), though their structure is very well conserved. An integrin molecule is an heterodimer composed of two noncovalently associated glycoprotein subunits, called α and β. In humans, eighteen different α and eight β subunits have been described. Combined in different associations they favor the activation by specific signals and the membrane transfer of different messages. Moreover, those combination assemblements can allow the formation of junctions either small and transient or large and durable. Both subunits span the cell membrane leaving out short intracellular C-terminal tails and large N-terminal extracellular domains.
The extracellular portion of the integrin dimer binds to specific amino acid sequences in extra cellular matrix proteins (such as laminin or fibronectin),

or to ligands on the surfaces of other cells. The intracellular portion binds to a complex of proteins that form a linkage to actin filaments of cytoskeleton. A key component for this linkage is talin. The incredible versatility of integrins requires a complex structure: they cannot simply be passive, rigid object with sticky patches at their two ends; oppositely, they must be able to rapidly make and brake attachments to the matrix in appropriate circumstances. Furthermore, the binding of their ligands on one side of the membrane must alter their propensity to bind a different set of ligands on the opposite side. The basis for these dynamic phenomena is allosteric regulation: as an integrin binds to or detaches from its ligands, it undergoes conformational changes that affect both the intracellular and the extracellular ends of the molecule. Structural change at one end is coupled to a structural change at the other. In this way, influences can be transmitted in either direction across the cell membrane. Effectively, an unusual feature which is peculiar to these kind of receptors is undoubtedly bidirectional signaling. As a matter of fact, these trans-membrane receptors are able to respond both to extracellular and intracellular stimuli thus signaling in both directions across the membrane.

As figure 1.1 shows, there are mainly two possible integrin conformations: a bent structure and an upright configuration. The bent one is usually taken to represent the inactive integrin state in which the probability to bind to the ligand is very low (still is not zero) Fig. 1.1 (A). The upright structures represent the intermediary state and the fully open state, respectevely Fig.1.1 (B) and Fig. 1.1 (C). In the intermediary state, ligand affinity is remarkably increased, whereas the fully open state corresponds to the active adhesive state. The activation process can be of the following types:

- Inside-out
- Outside-in

In the first case a signal generated inside the cell leads to increased affinity to the binding ECM ligand: talin binds the cytoplasmatic tail causing tail separation and distinct conformational changes in the integrin domains.
On the other hand, outside-in activation is brought as soon as the ligand binds to the integrin head leading both to conformational changes and integrin's clustering, or some combination of these. This finally results in intracellular change.

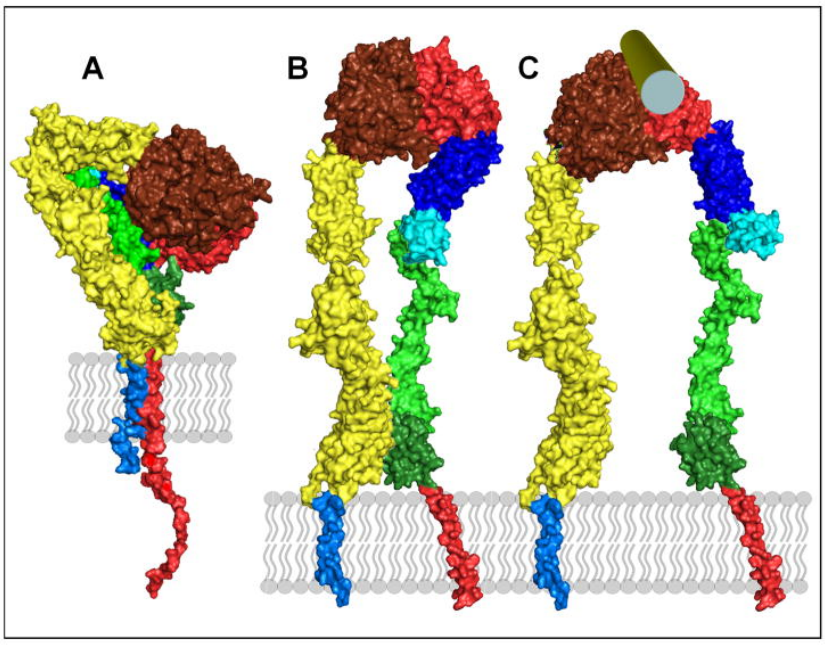

Figure 1.1: Schematic views of integrin conformations. (A) inactive state (B) A possible intermediate state (C) active state

Talin plays a key role also in outside-in signaling, by forming a direct linkage between the integrin and the actin cytoskeleton. The head region, where the α and β chains meet, contains the binding site for the extracellular ligand. Binding of the ligand distorts this region so as to favor adoption of the extended, active conformation; conversely, adoption of the extended conformation creates a more favorable binding site, with a higher affinity for the ligand. Then, the changes in extracellular region cause the events in the intracellular end of the integrin molecule. In its folded, inactive state, the intracellular portions of its α and β chains lie close together and adhere to one another. When the extracellular domain unfolds, this contact is broken and the intracellular (and transmembrane) portions of these chains move apart. As a result, a binding site for talin on the tail of the β is exposed. The binding of talin then leads to assembly of actin filaments anchored to the intracellular end of the integrin molecule. In this way, when an integrin catches hold of its ligand outside the cell, the cell reacts by tying its cytoskeleton to the integrin molecule, so that force can be applied at the point of attachment.
The chain of cause and effect can also operate in reverse, from inside to outside. Talin competes with the integrin α chain for its binding site on the tail of the β chain. Thus, when talin binds to the β chain it undoes the intracellular $\alpha - \beta$ linkage, allowing the two legs of the integrin molecule to spread apart. This drives the extracellular portion of the integrin into its extended, active conformation.
Both outside-in and inside out activations processes involve the regulated assembly and disassembly of a large number of components [1]. Integrins do not work in isolation; it is thanks to these time-dependent complexes that signaling can occur. Changes in the heterodimer are always linked to other processes, such as integrin clustering and the assembly of large intracellular adhesion complexes. They are composed by constituents known as adhesomes that form a network of 156 proteins, linked by many hundreds of protein interactions. It has been recently shown that many ligands proteins are able to bind to the integrin tail [1]. Their role is obviously fundamental in the activation process.
Talin is a large protein which plays a key role in the integrin activation and in vertebrates is expressed in two isoforms: talin1 and talin2. The first one is expressed widely while the second one is primarily found in the striated muscle and in the brain. It has been shown that talin exists in several conformational states, monomer and dimer, as well as open and

auto-inhibited closed form. Auto-inhibited talin can be activated by the PIP_2 pathway [1].
There are several known triggers for integrin's activation and, among these, one of the most recognized in literature is the activation pathway involving phosphatidynositol $(4,5)$-biphosphate (PIP_2) and calpain, intracellular regulatory molecules that trigger the "inside-out" activation.
The local concentration of PIP_2 is increased by the activity of phosphatidynositol phosphate kinase type I (PIPKI) enzyme leading to the association of talin to the integrin β tail. In this way, a signal generated inside the cell can trigger its integrin molecules to reach out and grab hold of their extracellular ligands. Intracellular signal molecules, such as PIP_2 are themselves produced in response to signals received from outside the cell via other types of cell-surface receptors. In this way they control integrin activation following the model reception-transduction-response. Conversely, the activation of integrins by attachment to matrix can influence the reception of signaling by other pathways. The cross-talk between all these communication pathways, transmitting signals in both directions across the cell membrane, allows for some complex interactions between the cell and its physical/chemical environment. Moreover, it allows the production of signals that can influence almost any aspect of cell behavior, from proliferation and survival, (as in the phenomenon of anchorage dependence of cellular growth) to cell polarity and guidance of migration.

1.2 Proposal

Obviously, mathematical modeling cannot provide an answer to all questions posed by biochemistry. However, modelling can help us to understand the physical strategies used by biological systems to build complex macro-structures such as adhesive complexes [1]. These macro-structures are reminiscent of some localized self-sustained structures studied in abstract dynamical systems, and these solutions depend on key properties such as characteristic diffusion lengths and characteristic time scales. In order for the model to be amenable for analysis, we will need to simplify the biological reality and we will only retain the essential features. In what follows, we will consider integrin receptors as two-state systems which can be either in their inactive or active conformational state. The

fractional population between the two states will depend on the concentration of an abstract field $u(x,t)$, which mimics the crucial role of PIP_2. The signalization platform corresponding to an integrin with a partner protein to synthesize PIP_2 will also be considered via an abstract partner $v(x,t)$. In order to accomplish this task, I would employ computational modelling as a tool to draw deeper understanding of the studied system. The final hope is that the predictions generated by these techniques and simulations with these models can be experimentally tested and provide new insights into the biological processes. In order to achieve this, I will take as an example the Gray-Scott reaction-diffusion model (see Chapter 4) which permits to build up a model of differential equations once that the chemical reactions and their taxes are known. Once that part is done, I use the techniques of dynamical systems to find out stationary particular solutions. A fundamental property of these solutions is that they describe localized states of matter characteristic of out-of-equilibrium systems.

Chapter 2

Biomathematics

In this brief chapter we shortly point out some matters such as when and how mathematics has joined the study of life. Therefore we try to answer questions like what are, and why are mathematical models needed in Biology. Finally we outline the basics of modelling highlighting some recurrent phenomena and the basic definitions.

2.1 The role of math models in biology

In this biological context, one can explore the use of contemporary mathematical modelling techniques in order to describe the biological mechanisms portrayed in the previous sections. Mathematical systems are currently becoming more and more popular in molecular biology research. These systems approches stand on the opposite side with respect to the traditional biology. The very gradual shift between these two perspectives passed a turning point at the end of the twentieth century, when brand new experimental techniques provided system level observations of cellular networks. These observations reported the nontrivial full complexity of these networks showing that the ordinary qualitative biology techniques were ill-defined for the investigation of these systems. This point was wisely explained by Yuri Lazebnik in his *gedankenexperiment* [7]. He described a (failed) attempt to reverse-engineer a transistor radio using qualitative methods analogous to those used in traditional molecular biology. Lazebnik's mental experiment shows that without a quantitative framework to describe large networks of interacting components, the

functioning of cellular network cannot be resolved.
A quantitative approach to molecular biology allows traditional interaction diagrams to be extended mechanistic mathematical models. These models works as an hypotheses: they help to understand and predict the behaviour of complex systems.
This application of mathematical methods to molecular cell biology is not a new effort. There is a long hystory of mathematical descriptions of biochemical and genetic networks. Among these successful applications we find Alan's Touring's description of patterning in development [10], the models of neuronal signaling developed by A. Hodgkin and Huxley [14] and the mechanistic modelling of the heart by Denis Noble [12]. Despite these successes, this sort of mathematical work has not been considered central to most of cell molecular biology. Notwithstanding, the attitude is changing, system level investigations are now frequently accompanied by mathematical models, and such models might soon become a requisite for describing cellular networks.

2.2 Approaches of traditional biology

Mathematical models are, as all models, abstractions of reality. They are particularly designed to focus on certain aspects of the object under study, while other aspects are disregarded. For instance, the famous ball-and-stick model of the chemical structure focuses on the chemical bonds of a molecule, and it does not capture the resulting polarity of any of the involved atoms.

Biologists make use of tangible real world models regularly. These can be rather simple, such as the ball-and-stick model or complex such as model organisms or animal deseases. Biologists also use conceptual models. These, usually take the form of verbal description of systems, and are communicated by diagrams that illustrate a set of components and the ways in which they interact. These interaction diagrams, or cartoon models play a central role in representing our understanding of the cellular processes, see Fig. 2.1.
A defect of these cartoon networks is the ambiguity regarding system behaviour, especially when the interaction network involves feedback. By using a mathematical description of the system, we can eliminate that un-

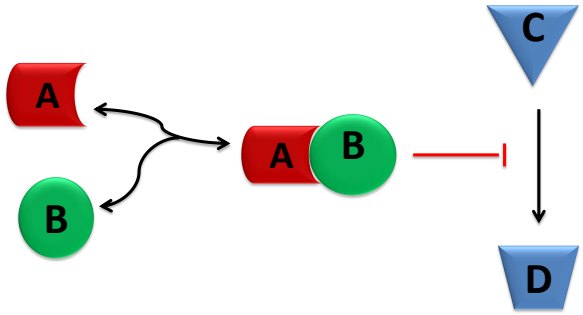

Figure 2.1: Interaction diagram in the form of a "Cartoon Model". Molecular species A and B bind reversebly to form a molecular complex. This complex form inhibits the rate at which molecules species C are converted to D. The blunt ended arrow indicates inhibition or repression. The red line indicates that this is a regulatory interaction in which the complex is not consumed.

certainty at the cost of demanding a quantitative representation of each interaction (interactions are represented by arrows in the cartoon model illustrated in Fig. 2.1). As an example, suppose that two species A and B bind to form a complex. In order to quantify that interaction, a numerical description of the process must be involved. For some uses, it may be sufficient to introduce the equiibrium constant for the reaction. In other cases, the rate of binding (association) and the rate of unbinding (dissociation) are needed. For a great many cellular processes, our current level of knowledge cannot support a quantitative description: we have only a qualitative understanding of the relevant molecular interactions. However for a growing number of well studied mechanisms, sufficient data has been collected to allow the quantitative characterization.
When the relevant data is known, the interaction diagram can be used to formulate the dynamical mathematical model. The model development process is described in Chapter 3 for the Gray-Scott Model and in Chapter

4 for the Integrin Model. Both models consists in a set of equations that describe how the system changes over time, i.e. the system dynamical behaviour.

2.3 Model's predictions

Quantitative descriptions of molecular interactions generally invoke the laws of physics and chemistry. The resulting models are called *mechanistic* ast they describe the mechanisms that drive the observed behaviour. Each component of a mechanistic model represent a certain aspect of the model under study. Modifications to the components of the model mimic modifications to the real system. Investigation of mechanistic models follow two complementary paths, **model simulations** and **model analysis**. The more direct approach is model *simulation* in which the model is used as a tool for predicting the system behaviour under given conditions. Simulations are sometimes referred to as *in silico* experiments, because let computers to mimic the behaviour of the biological system. They are carried by numerical simulation packages and they are heavily used in Chapter 5.
Alternatively, models can be investigated analytically, yielding general insights into their potential behaviour. These *model analysis* approaches involve sophisticated mathematical techniques. The advantage for mastering these techniques is an insight into the system that cannot be reached through simulation. While simulations indicate how a system behaves, model analysis reveals *why* a system behaves as it does. This analysis can reveal non-intuitive connections between the structure of a system and its consequent behaviour.

2.4 Complex systems features

Cells systems are usually classified as *complex systems*. Both the words *system* and *complexity* are usually overrated and they can be ambiguous in some contexts. The term *system* is often used without formal definition. Its meaning is in someway dependent of the context, but most of the times it refers to a collection of interacting objects. For example, a stone alone

is not considered a system but an avalanche of stones is; the stones in the avalanches "talk" to each other by pushing one other around [6]. Besides the multiple interacting components, the other defining feature of a system is the *boundary*. Having said that a system is a collection of components, anything that is not one of those components is not part of the system and so is part of the external environment. For instance, the cell membrane defines a boundary between the cell, as a system, and the extracellular environment. In certain contexts, a system is defined exclusively in terms of its interaction with this outside world, and it is then called *input-output system*.

Likewise, the word *complexity* is also overrated and it means different things to different people. Most would agree that a system qualifies as complex if the overall behaviour of the system itself cannot be intuitively understood in terms of the individual components or interactions. A defining feature of complex systems is that the qualitative nature of their behaviour can depend on quantitative differencies in their structure. In other words, behaviour can be drastically altered by seemingly insignificant differences in system features.

Two essential features of complex systems are nonlinear interactions and feedback loops. The latters can be either *negative* or *positive*, as the one involving the activator and the inhibitor presented in Chapter 4.

Negative feedback is exhibited when system components inhibit their own activity. A familliar example is the household thermostat that corrects for deviation of temperature from a set point. These feedback loops generally stabilize system behaviour being the key feature of self regulation and homeostasis. However, instability and oscillation can arise when there is a lag in the action of a negative feedback loop.

Positive feedback is generally associated with unstable divergent behaviour. An example is the runaway screech that occurs when someone brings the guitar close to the speaker enclosure of the guitar amp. However, when constrained by saturation effects, positive feedback can serve as a mechanism to locked in a system long-term behaviour thus allowing a cell of retaining a memory of past conditions.

Since a model is a hypotheses, the results of model investigation are themselves hypotheses. Simulations cannot definetively predict cellular behaviour, but they can serve as valuable guide to experimental designs, by indicating promising avenues for further investigations, or by revealing inconsistencies between our understanding of a system (embodied in the

model) and laboratory observations. In fact, the identification fo such inconsistencies is a key benefit of modelling. As a model can be exhaustively investigated, it follows that a negative result - the inability of a model to replicate eperimental observations - can be taken as a falsification of the hypotheses on which the model was built. This process of autoconsistency can lead to a refinement of the biological hypotheses, and subsequently to a refined model, which can be tested against additional experiments. This iterative process results in a continuous improvement in the understanding of the system called virtuous cycle. The end goal of most modelling efforts is a fully predictive description; simulations are then guaranteed to be accurate representation of real behaviour.

2.4.1 Basic Modelling features and definitions

The basic components of a dynamic mathematical model correspond to the molecular species involved in the system. For each species a state variable is assigned. The collection of all these state variables is called the *state* of the system. The state of the system provides a complete description of the condition of the system at any given time. The dynamic behaviour of the model is the time-course for the collection of state variables.
Besides the variable of states, models inculde also parameters, whose values are fixed. Model parameters characterise interactions among the components of the system and with the environment. Examples of parameters are: association constants, maximal expression rates, degradation rates and buffered molecular concentrations. A change in the value of the model corresponds to a change in an environmental condition or on the system itself. For this reason, parameters are held constant during simulations. These values can be varied to explore system behaviour under perturbations or in altered environments such as different experimental conditions. For any given model, the distinction between the state variables and the model parameters is clear cut. However, this distinction depends on the context and on the time scale over which simulations run.
Simulations of dynamic models represent time varying system behaviour. Models of biological processes almost always arrive, in the long run, at steady behaviours. Most commonly, models exhibits a persistent operating state, called a **steady state**; some systems display sustained oscillations. The time-course that leads from the initial state to the long-time (or

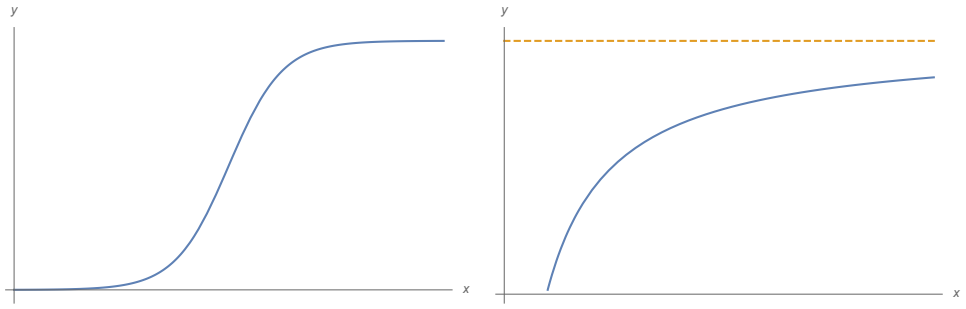

(a) s-shaped curve (b) hyperbolic saturation

Figure 2.2: Typical nonlinear curves behaviour in biological processes. In Hyperbolic saturation Fig. 2.2b as x incerases y increases but at an ever-diminishing rate. For x tending to infinity the y approaches the asymptotic value, dashed yellow line in Fig. 2.2b. In Sigmoidal nonlinearity y shows a slow rate of increase for small x. Then a rapid "switch-like" rise toward the limiting value follows.

asymptotic) behaviour is referred to as the **transient**. In some cases, one will rather focus on transients behaviour as it reflects the immediate response of a system to perturbation just like in the first sections of Chapter 5. In other cases, one may analyse only the steady state as it reflects the prevailing condition of the system over significant stretches of time.

Another ingredient typically involved in cell biological processes is nonlinearity. Nonlinear relationships do not need to follow any specific pattern and so are generally difficult to address with any generality. The ones that appear mostly in biochemical and genetic interactions are saturations, in which one variable increases with another at a diminishing rate, so that the dependent variable tends to a limiting or asymptotic value. In Fig. 2.2, two kinds of saturation curves commonly encountered in biology.

Another important aspect in the study of nonlinear models is the wide range of behaviours that can be exhibited. In most cases, an overall, global detailed analysis is overwhelming. Instead, attention can be focused on specific aspects of system behaviour near particular operating points. In this operation, one can take advantage of the fact that nonlinear relationships can always be linearly approximated in the small domains. This local approximation allows the application of the tools typical of linear analysis. Still, as intuition suggests, this approach is too handicapped to

be of much of use. However, the global behaviour of systems is often tightly constrained by their behaviour around some nominal operating points. Local analysis at these points can therefore provide comprehensive insight ito the global behaviour.
Mathematical models can be further classified into deterministic and stochastic. The notion of determinism-reproducibilty of behaviour-is a foundation for much of scientific investigation. A deterministic model in the very same logic is simply a model whose behavour is exactly reproducible.
Although the behaviour of a deterministic model is dependent upon a specific set of conditions, no other forces have any influence so that repeated simulations under the same conditions are always in perfect agreement.
On the other hand, stochastic models allow for randomness in their behaviour. The behaviour of a stochastic model is influenced both by specified conditions and unpredictable forces. Repeated stochastic simulations thus yield distinct samples of system behaviour [4].

Chapter 3

The Gray-Scott Model

In this chapter we take a brief insight into the model of a continuously fed unstirred autocatalytic reaction (CFUR) due to Gray and Scott [13]. In this CFUR model, two chemical species A and B are involved in the simplest of the circumstances, i.e., uniform temperatures and homogeneous concentrations. The model involves what are called *quadratic autocatalysis* and *cubic autocatalysis*, whose reaction schemes are given by:

- quadratic autocatalysis $A + B \to 2B$,
- cubic autocatalysis $A + 2B \to 3B$,

where the catalyst may be stable or have a finite lifetime. Studying these reactions, confrontation with miscellaneous phenomena arises. Among these we have multistability, critical extinction, critical ignition and anomalous relaxation times (though infinite values are not reached). When looking for stationary patterns isolas and mushrooms occur. This singular behaviour is given by the presence of the catalyst B in the inflow.

3.1 Stechiometry kinetics

The simplest form of autocatalytic reactions can be expressed by the prototype reaction steps:

$$A + B \to 2B \tag{3.1}$$
$$A + 2B \to 3B \tag{3.2}$$

Both reactions are represented by the $A \rightarrow B$ stoichiometry, but the reactions rate depends differently on the concentration of the product species B, viz.

$$\tau = \alpha[A][B]^n, \qquad n = 1, 2. \tag{3.3}$$

Hence, one can refers either to the quadratic (or simple) autocatalysis ($n = 1$), or to the cubic autocatalysis ($n = 2$). Generally, in closed systems the reaction rate rises to a maximum and then falls to zero as the equilibrium is reached. This results in a S-shaped curve of product concentrations vs time. As illustrated in Chapter 2, these curves are very common in many biological systems such as population growth in a limited food supply, or spread of infectious diseases. Nevertheless, it may occur in gas-solid reactions and solid-solid transitions where the rate is proportional to the contact surface between the two phases.

3.1.1 Simple autocatalytic or quadratic reaction

In the simple autocatalytic reaction $(n = 1)$ we have

$$\frac{db}{dt} = kab - k_{res}b, \tag{3.4}$$

where k is the reaction rate constant and $k_{res} = 1/t_{\text{res}}$ is the inverse of the residence time t_{res} which plays the role of a first order rate-constant. In equation (3.4) it is assumed that the concentration of B in the inflow is zero, $b_0 = 0$. Conveniently, one may choose adimensional constants, viz.

$$\gamma = \frac{a - a_0}{a_0} \qquad \text{or} \qquad \gamma = \frac{b}{a_0} \tag{3.5}$$

these definitions are equivalent as long as we have the further constraint

$$a + b = a_0. \tag{3.6}$$

Therefore, a and b cannot actually vary independently. We are then left with only one independent variable. In dimensionless terms we find

$$\frac{d\gamma}{dt} = \gamma ka - \gamma k_{res}. \tag{3.7}$$

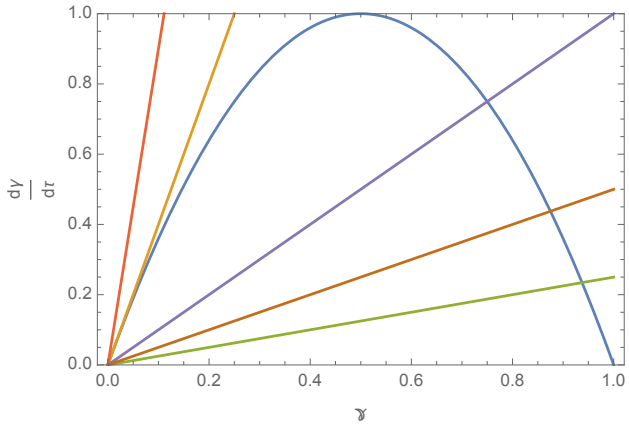

Figure 3.1: Rate of production and rate of loss curves for quadratic autocatalysis

Introducing the following change of variable:

$$\tau = \frac{t}{t_{\text{chem}}},$$

where τ is the dimensionless time and the chemical time t_{chem} is chosen to be

$$t_{chem} = \frac{\text{initial conc. of A}}{\text{maximum chemical reaction rate}} = \frac{a_0}{\frac{1}{4}ka_0^2} = \frac{4}{ka_0} \tag{3.8}$$

we therefore have,

$$\frac{d\gamma}{d\tau} = 4\gamma(1-\gamma) - \gamma/(Da); \tag{3.9}$$

where the group Da represents a dimensionless residence time

$$(Da) = \frac{t_{\text{res}}}{t_{\text{chem}}}. \tag{3.10}$$

The factor 4 in the first member on the r.h.s. of equation (3.9), the chemical rate of production of B, $(d\gamma/d\tau)_{\text{chem}}$, occurs so that this production rises to a maximum of unity. On the other hand, the second member on the r.h.s of equation (3.9) represents the rate of outflow of B, $(d\gamma/d\tau)_{\text{flow}}$.

Plotting both rates as functions of γ, Fig. 3.1, we notice that the loss line is a straight line of gradient $1/Da$ while the production curve is a parabola

reaching its maximum for $\gamma = 1/2$. For long residence times or slow flowrates, the loss lines have slow slope. For slow flow rates, e.g. $Da < 1/4$, there are two intersections; one at $\gamma_1 = 0$ and another one given by

$$\gamma_2 = 1 - \frac{1}{4Da}. \tag{3.11}$$

As a matter of fact, we have two stationary-state solutions; the one with subscript 1, the lowest, and the ones with subscript 2 (or more than 2 in general which indicates other solutions in order of increasing γ). As Da tends to $1/4$, the two solutions converge at $\gamma_1 = 0$. For faster flowrates, the nonzero intersection becomes negative and is not physical. The following multistability condition is founded for

$$Da > \frac{1}{4} \qquad \text{or} \qquad t_{\text{res}} > \frac{1}{ka_0}. \tag{3.12}$$

3.1.2 Cubic autocatalysis

Similiarly, we can perform the same procedure for the cubic autocatalysis, obtaining

$$\frac{db}{dt} = kab^2 - k_{res}b, \tag{3.13}$$

which in dimensionless parameters reads

$$\frac{d\gamma}{d\tau} = \frac{27}{4}\gamma^2(1-\gamma) - \gamma/(Da). \tag{3.14}$$

The normalizing factor, $27/4$, occurs because the maximum of the production rate is $4/27$, which is found for $\gamma = 2/3$. The chemical time t_{chem} contains that factor

$$t_{\text{chem}} = \frac{a_0}{\frac{4}{27}ka_0^3}; \tag{3.15}$$

hence

$$Da = \frac{4}{27}ka_0^2 t_{\text{res}}, \quad \tau = \frac{4}{27}ka_0^2 t. \tag{3.16}$$

The cubic rate of production curve as a function of γ passes through zero at $\gamma = 0$, afterwards showing an inflexion point at $\gamma = 1/3$; it reaches a maximum at $\gamma = 2/3$ and falls to zero at $\gamma = 1$. The rate of removal is a straight line with gradient $(Da)^{-1}$ just as before. In the slow flowrate

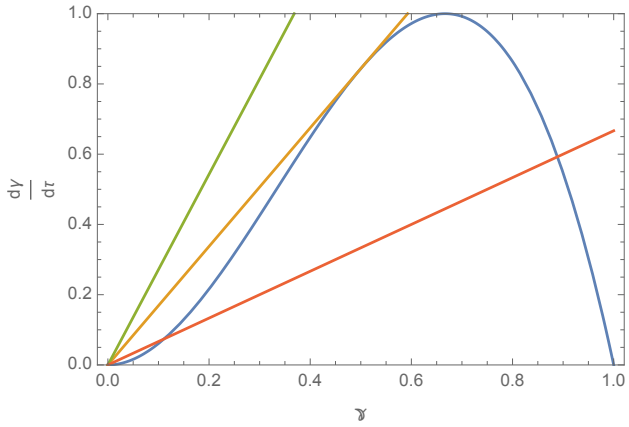

Figure 3.2: Rate of production and rate of loss curves for cubic autocatalysis.

regime there are three intersections and therefore three stationary-state solutions. One is at $\gamma_1 = 0$, the second one is in the range $0 < \gamma_2 < 1/2$ and the third one is in the range $1/2 < \gamma_3 < 1$. As the flow rate increases the two nonzero intersections move closer and closer finally merging in $\gamma = 1/2$, while the loss line becomes tangential to the production curve when $Da = 16/27$. For higher flow rates, the nonzero solutions disappear and the reaction is extinguished. The condition for multistability is

$$Da > \frac{16}{27} \quad \text{or} \quad \frac{1}{4} t_{\text{res}} > \frac{1}{k a_0^2}. \tag{3.17}$$

The nonzero intersections are given by the quadratic equation

$$\gamma_{2,3} = \frac{1}{2}\left[1 \pm \sqrt{1 - \frac{16}{27}(Da)^{-1}}\right]; \quad \gamma_1 = 0. \tag{3.18}$$

3.2 Stability of stationary states

Perturbing a steady-state by a small amount $\Delta\gamma_0$, then variation of this displacement in time $\Delta\gamma$ will be given by

$$\frac{d\Delta\gamma}{d\tau} = \lambda\Delta\gamma + \mu(\Delta\gamma)^2 \tag{3.19}$$

where the coefficients

$$\lambda = \frac{\partial}{\partial\gamma}\frac{d\gamma}{d\tau} \quad \text{and} \quad \frac{1}{2}\frac{\partial^2}{\partial\gamma^2}\frac{d\gamma}{d\tau} \tag{3.20}$$

are evaluated at the stationary-state. Considering the small perturbations such that

$$\left|\mu\left(\Delta\gamma_0\right)^2\right| \ll |\lambda\Delta\gamma_0| \tag{3.21}$$

the displacement at any time τ is then given by

$$\Delta\gamma(\tau) = \gamma - \gamma_{ss} = \Delta\gamma_0 \exp(-\tau/\tau^*) \tag{3.22}$$

where $\tau^* = -1/\lambda$. We therefore have:

- $\lambda < 0 \Rightarrow$ stable
- $\lambda > 0 \Rightarrow$ unstable
- $\lambda = 0 \Rightarrow$ special case

In the last case, $\lambda = 0$, production and loss lines intersect tangentially, and τ^* is apparently infinite. However, in this special case a further analysis is required as the condition of small perturbations (3.21) is no longer satisfied. In the simple quadratic autocatalysis we have

$$\lambda_1 = 4 - (Da)^{-1}, \quad \text{at} \quad \gamma_1 = 0 \tag{3.23}$$

$$\lambda_2 = -\left(4 - (Da)^{-1}\right), \quad \text{at} \quad \gamma_2. \tag{3.24}$$

As expected, λ_1 and λ_2 have opposite signs so that γ_1 and γ_2 have opposite stability. When γ_2 is positive it is stable because λ_2 is negative; λ_1 is then unstable. If Da is less than $1/4$, so that only γ_1 is physically realistic, λ_1 is positive so that the origin is stable. For the cubic autocatalysis we obtain from equation (3.14)

$$\lambda_1 = -(Da)^{-1} \quad \text{at} \quad \gamma_1 \tag{3.25}$$

$$\lambda_2 = \frac{27}{4}\gamma_2\left(1 - 2\gamma_2\right) \quad \text{at} \quad \gamma_2 \tag{3.26}$$

$$\lambda_3 = \frac{27}{4}\gamma_3\left(1 - 2\gamma_3\right) \quad \text{at} \quad \gamma_3 \tag{3.27}$$

Thus, γ_1 occurring at the origin is always stable for any flow-rates because λ_1 is always negative. The second solution γ_2 lies between 0 and 1/2 so it is unstable because λ_2 is positive. The third intersection γ_3 is stable as λ_3 is negative. When $Da = 16/27$ and $\gamma_2 = \gamma_3 = 1/2$, λ_2 and λ_3 become zero; as a result, the exponential form of equation (3.22) no longer holds.

3.3 Product inflow

Among the stationary-states in autocatalysis we have the zero reactant conversion, $\gamma = 0$. However, there is no reason for which the reaction can get started and then move on one of the other stationary states. This is equivalent in finding an infinite induction period in a closed-vessel. This "nucleation problem" can be avoided letting fall the hypotesis of zero concentration of B in the inflow.

3.3.1 Inflow contains catalyst in simple autocatalysis

The dimensionless mass-balance equation can be written as

$$\frac{d\gamma}{d\tau} = 4(\gamma + \gamma_0)(1 - \gamma) - \frac{1}{Da}\gamma, \tag{3.28}$$

where $\gamma_0 = b_0/a_0$, which typically is around 10^{-6}.

The rate of production is positive and nonzero when $\gamma = 0$;i t rises to a maximum at $\gamma = 1/2(1 - \gamma_0)$ finally falling to zero (complete conversion) at $\gamma = 1$. Compared to the precedent case, the maximum is shifted from $\gamma = 1/2$ by an amount $1/2\gamma_0$. Moreover, near the origin there is no more solution at $\gamma = 0$, and there is one and only one intersection over the range $0 \leq \gamma \leq 1$, for any positive flow rate. This unique stationary state solution is stable as the corresponding λ is negative.

3.3.2 Inflow contains catalyst in cubic autocatalysis

Mass-balance equation in the cubic autoctalysis takes the form

$$\frac{d\gamma}{d\tau} = \frac{27}{4}(\gamma + \gamma_0)^2(1 - \gamma) - \frac{1}{Da}\gamma. \tag{3.29}$$

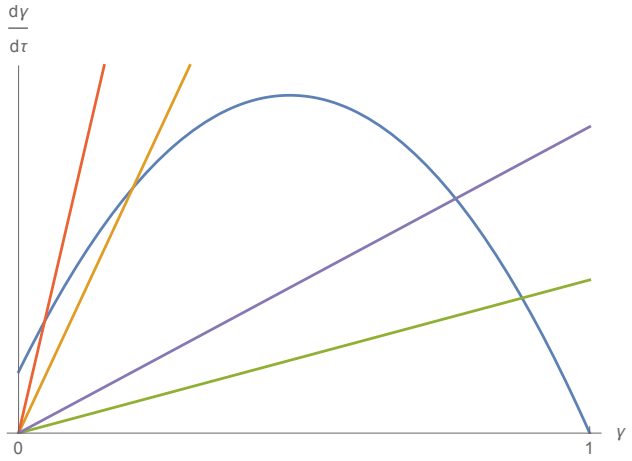

Figure 3.3: Rate of production and loss lines for product inflow

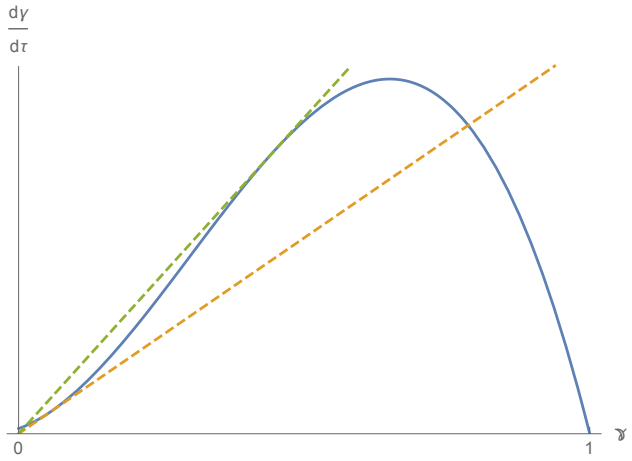

Figure 3.4: Rate of production and loss lines for product inflow in cubic autocatalysis

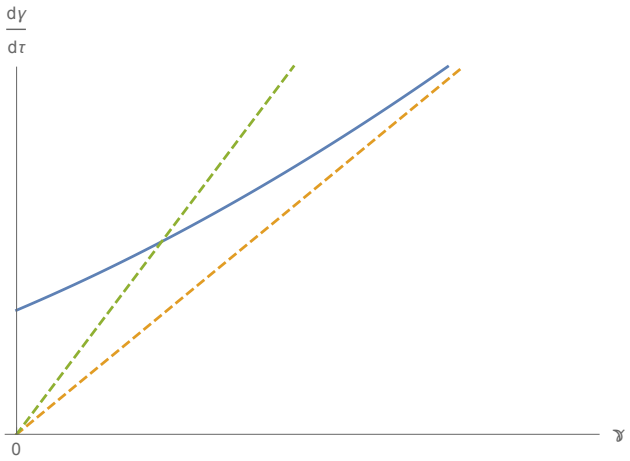

Figure 3.5: Rate of production and loss curves for cubic autocatalysis with product inflow

Again, $\gamma = 0$ is not a solution of the stationary state condition $\frac{d\gamma}{d\tau} = 0$ as shown in Fig. 3.5, which is a zoom near the origin of Fig. 3.4.

The inflexion in the production curve is now $\gamma = 1/3 - 2/3\gamma_0$ while the maximum occurs at $\gamma = 2/3 - 1/3\gamma_0$. More than one tangent to the production curve are allowed and there will be either one or three intersection in the positive quadrant, as shown in Fig. 3.4. Tangency occurs at

$$\gamma_{\pm} = \frac{1}{4}\left[1 \pm \sqrt{1 - 8\gamma_0}\right], \tag{3.30}$$

where the minus sign corresponds to *ignition*, while the upper root corresponds to *extinction*. If $\gamma \ll 1$ then ignition occurs at

$$\gamma_{\text{ign}} \simeq \gamma_0, \tag{3.31}$$

while extinction occurs at

$$\gamma_{\text{ext}} \cong \frac{1}{2} - \gamma_0. \tag{3.32}$$

As the concentration of the autocatalystic species in the inflow increases and $\gamma_0 \to \frac{1}{8}$ the ignition and extinction points merge and multistability disappears. If we restrict ourselves to small values of γ_0, say $\gamma_0 \ll 1/8$, then the range of residence times over which multistability occurs is given

by

$$\frac{16}{27(1+4\gamma_0)} \leq (Da) \leq \frac{1}{27\gamma_0(1-2\gamma_0)}. \tag{3.33}$$

3.4 Exotic behaviour

Until now, only isothermal autocatalysis with perfectly stable catalytic product has been considered. In real systems, catalysts do not remain unchanged. The simplest representation of catalyst decay is

$$B \rightarrow \text{products} \qquad \text{rate} \propto [B]. \tag{3.34}$$

When this possibility is taken into account, phenomenas associated with self heating and heat losses or with very complex isothermal kinetics can be found. Among these, we find isolas, mushrooms and sustained oscillations. Here, we have to decouple the concentrations A e B which have been previously linked with by equation (3.6). This decoupling is automatic if the autocatalytic species B is not perfectly stable, but undergoes decay, either homogeneously or heterogeneously. We are then led to the following reaction schemes

$$A + nB \rightarrow (n+1)B \quad \text{rate} = k_1 a b^n, \tag{3.35}$$

$$B \rightarrow \text{inert} \qquad \text{rate} = k_2 b, \tag{3.36}$$

where $n = 1, 2$. As the species B is no long indefinitely stable, the simple relationship (3.6) does not hold anymore and therefore the two possibilites for the choice for the dimensionless measure of extent of reaction

$$\gamma = \frac{a_0 - a}{a_0} \quad \text{or} \quad \gamma = \frac{b}{a_0} \tag{3.37}$$

are no longer equivalent, nor even simply related.

3.4.1 Simple quadratic catalysis with decay

In the simple catalysis, the two mass balance equations read

$$\begin{cases} \dfrac{da}{dt} &= -k_1 ab + k_{\text{res}}(a_0 - a) \\ \dfrac{db}{dt} &= k_1 ab - k_{\text{res}}(b_0 - b) - k_2 b. \end{cases} \tag{3.38}$$

In the stationary state, both time derivatives vanish and we can combine eq.ns (3.38) obtaining the extra condition

$$b_{ss} = \frac{k_{res}}{k_2 + k_{res}}(a_0 + b_0 - a_{ss}). \tag{3.39}$$

Clearly, this equation applies only to the stationary state and recovers the former case Eq. (3.6) when k_2 tends to zero. Considering the dimensionless residence-time and reaction-time for step 2, respectively

$$\tau_{res} = k_1 a_0 t_{res} \tag{3.40}$$

$$\tau_2 = k_1 a_0 t_2 = k_1 a_0 / k_2, \tag{3.41}$$

assuming $b_0 = 0$ and substituting equation (3.39) in the first of eq.ns (3.38) we obtain

$$\gamma_{ss}(1 - \gamma_{ss}) - \frac{\gamma_{ss}}{\tau_{res}}\left(\frac{\tau_{res}}{\tau_2} + 1\right) = 0. \tag{3.42}$$

One solution is $\gamma_{ss} = \gamma_1 = 0$ as previously found, for the non zero stationary -state one can divide each member by γ_{ss} obtaining

$$\gamma_2 = 1 - \frac{1}{\tau_2} - \frac{1}{\tau_{res}}. \tag{3.43}$$

As τ_2 is not zero, this second intersection γ_2 cannot reach the unity even if the residence time becomes infinity. Moreover, there is also a lower limit on τ_{res} for γ_2 to stay positive which depends on τ_2. The value of γ_2 increases monotonically as τ_{res} decreases. Fig. 3.6 shows the flow diagram corresponding to Eq. (3.42); the loss line has a gradient of $1/\tau_{res} + 1/\tau_2$ which tends to $1/\tau_2$ as τ_{res} tends to infinity. If we consider a non-zero inflow of b ($\gamma_0 > 0$), again multistability is removed.

3.4.2 Cubic autocatalysis with decay

For cubic autocatalysis we have

$$\begin{cases} \dfrac{da}{dt} &= -k_1 a b^2 + k_{res}(a_0 - a) \\ \dfrac{db}{dt} &= k_1 a b^2 - k_{res}(b_0 - b) - k_2 b. \end{cases}$$

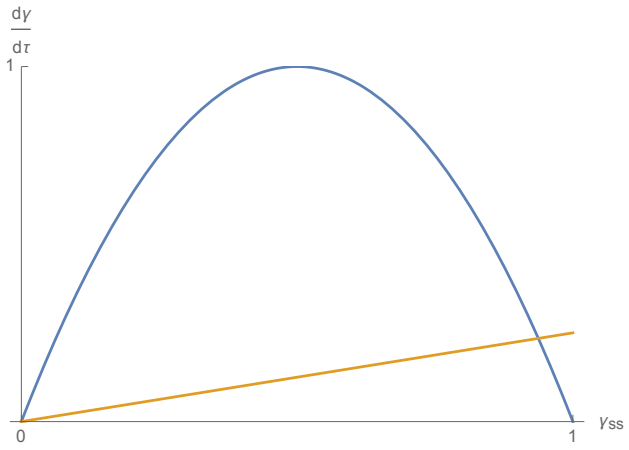

Figure 3.6: Flow diagram for simple autocatalysis with decay.

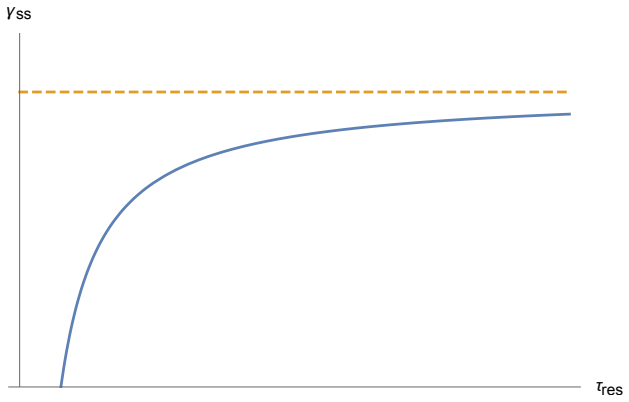

Figure 3.7: Non-zero inflow solution for quadratic autocatalysis with deacay.

Also in the cubic autocatalysis, the relationship Eq. (3.39) between a_{ss} and b_{ss} holds still. In the simpler case $b_0 = 0$ we have

$$\gamma_{ss}^2(1-\gamma_{ss}) - \frac{\gamma_{ss}}{\tau_{res}}\left(\frac{\tau_{res}}{\tau_2}+1\right)^2 = 0, \tag{3.44}$$

where

$$\tau_{res} = k_1 a_0^2 t_{res}; \tag{3.45}$$

$$\tau_2 = k_1 a_0^2/k_2. \tag{3.46}$$

We have a higher power in γ_{ss} in the first term, the chemical production rate in the stationary-state. In the rate of removal, we have also a higher power the latter being quadratic in τ_{res}.
Again, $\gamma_1 = 0$ is stationary solution, while the other two are given by the roots of

$$\gamma_{ss}(1-\gamma_{ss}) = \frac{1}{\tau_{res}}\left(\frac{\tau_{res}}{\tau_2}+1\right)^2. \tag{3.47}$$

Over some range conditions, Eq. (3.47) may yield *two* possible residence-times for a given value of γ_{ss} and *two* stationary state conversions, γ_2 and γ_3, for a given value of τ_{res}. The multiplicity of solutions of τ_{res} is a new feature not occurring in the stable case ($k_2 = 0$).
The condition of existence of the multiplicity over some range of γ_{ss} and τ_{res} is

$$\frac{1}{4} > \frac{4}{\tau_2}, \quad \text{i.e.} \quad k_2 < \frac{1}{16}k_1 a_0^2. \tag{3.48}$$

This condition arises because the maximum of the l.h.s. of Eq. (3.47) is $1/4$ (occurring for $\gamma_{ss} = 1/2$), and the minimum of the r.h.s of Eq. (3.47) as τ_{res} varies is $4/\tau_2$ (occurring for $\tau_{res} = \tau_2$).
When the inequality (3.48) is satisfied, the second and the third stationary-states lie on a closed cuve or isola, see Fig. 3.9. The existence of the isola and its size can be illustrated in the diagram flow of Fig. 3.8 corresponding to Eq. (3.44). As shown in Fig. 3.8, the production curve has the characteristic cubic form, and the loss line is linear in γ with a gradient related to τ_{res}. The smaller the residence-time, the steepest is the gradient. On the other hand, long residence-times reduce the steepness, but the gradient cannot be zero as it did in the stable case in absence of product decay. Instead, it has a minimum value of $4/\tau$ when $\tau_{res} = \tau_2$. The

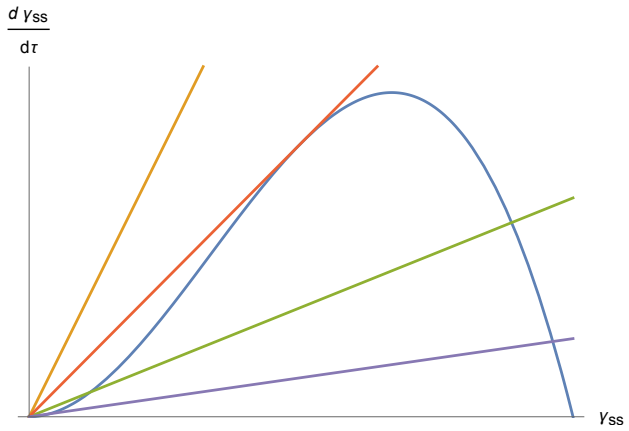

Figure 3.8: Non-zero inflow solution for cubic autocatalysis.

non-zero solutions range goes from the red tangent line in Fig.3.8 occurring for a gradient of $1/4$ until a gradient of 4τ. Moreover, the value of the gradient determines the number of possible intersections and then the pattern of depenence of γ_{ss} on τ_{res}. Here, miscellaneous possibilities are allowed. When the inequality (3.48) is not satisfied, the loss line of minimum slope is the one in orange in Fig. 3.8. The gradient of this line is greater than $1/4$, and the only intersection occurs at the origin, $\gamma_1 = 0$. Hence, the stationary-state solution is unique and zero for all residence-times. If (3.48) becomes an equality, multistability is still not allowed and the solution is the red tangent of the production curve in Fig. 3.8. Again, $\gamma_1 = 0$ is solution for all residence-times, but there is a second solution $\gamma_2 = 1/2$ at $\tau_{res} = \tau_2$. This represents the onset of multistability and the "birth" of the isola, Fig. 3.9. When the inequality (3.48) is satisfied, the loss lines lie below the tangent. For very short residence times, the slope of the loss line is very steep and it intersects the production curve only at the origin. As the residence time increases, the loss line slope decreases until becoming tangent when has a gradient equal to the red line shown in Fig. 3.8. Here in tangency, a second intersection occurs $\gamma_2 = \gamma_3 = 1/2$. Further increase of the residence times causes the loss line to become flatter (the green line in Fig. 3.8) and three intersections appear. When $\tau_{res} = \tau_2$, the slope reaches its minimum value (the violet line in Fig:3.8). Further increase of residence time will result in the above sequence to be retraced in re-verse so that the second and the third intersections come close together

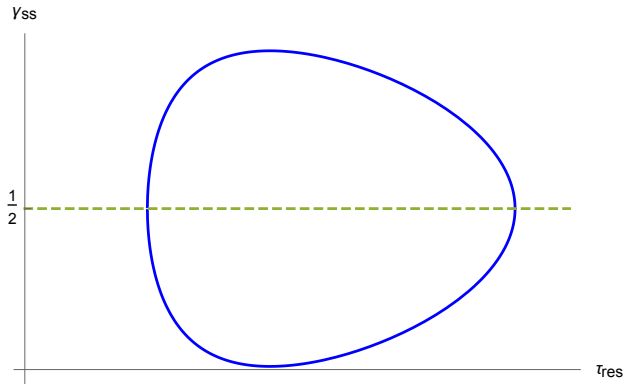

Figure 3.9: γ_{ss} plotted versus the residence time τ_{res} giving the closed curve called the isola

until finally merging at the tangency, $\gamma_2 = \gamma_3 = 1/2$. Hence, the resulting isola shown in Fig. 3.9 is symmetrical about $\gamma_{ss} = 1/2$ and it covers the widest range when $\tau_{res} = \tau_2$.
The isola extends over a range of residence times $\tau_{res}^{-} \leq \tau_{res} \leq \tau_{res}^{+}$, where $\tau_{res}^{\pm}$ represent the residence-times for which the slope of the loss line is equal to the tangent slope, i.e. for which

$$\frac{1}{\tau_{res}}\left(\frac{\tau_{res}}{\tau_2}+1\right)^2 = \frac{1}{4}, \tag{3.49}$$

which yields

$$\tau_{res}^{\pm} = \tau_2\left[\frac{1}{8}\tau_2 - 1 \pm \sqrt{\tau_2\left(\frac{\tau_2}{16}-1\right)}\right]. \tag{3.50}$$

Including the inflow of the autocatalytic species B, and denoting $\gamma_0 = a_0/b_0$, the stationary-state relationship becomes

$$(\gamma_{ss}+\gamma_0)(1-\gamma_{ss}) = \frac{1}{\tau_{res}}\left(\frac{\tau_{res}}{\tau_2}+1\right)^2\gamma_{ss}. \tag{3.51}$$

The production curve has two tangencies, occurring for small γ_0 ($\gamma_0 < 1/8$). Slopes of the tangent lines are $4\gamma_0(1-2\gamma_0)$ and $1/4+\gamma_0$. The relative position of these two tangents and the loss line of minimum slope do determine the nature of the $\gamma_{ss} - \tau_{res}$ diagram. The minimum slope of the

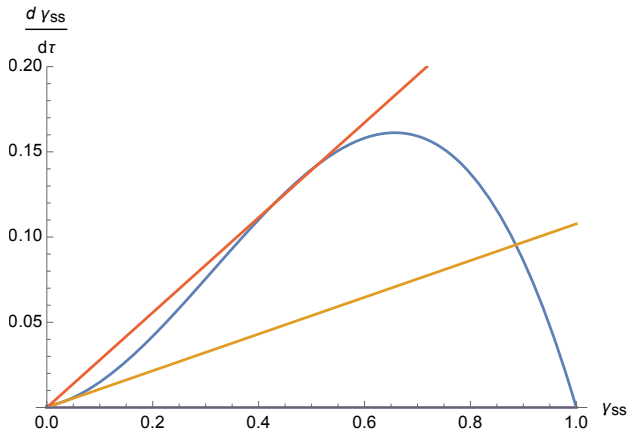

Figure 3.10: Inflow diagram: the production curve and the two tangent loss lines.

removal line is again $4/\tau_2$, occurring at $\tau_{res} = \tau_2$.
If the minimum slope is greater than the one of the upper tangent, only one intersection exists which lies close to the origin. This is shown in Fig. 3.11a.

The onset of an isola (Fig. 3.11b) occurs again when the loss line has a minimum slope equal to the upper tangent in Fig. 3.10.
If the loss line of minimum slope lies between the two tangent curves, i.e.

$$4\gamma_0(1-2\gamma_0) < 4/\tau_2 < 1/4+\gamma_0, \tag{3.52}$$

then the $\gamma_{ss} - \tau_{res}$ diagram exhibit isola behaviour, Fig.3.11c. The isola has two extinction points corresponding to the loss line crossing the upper tangent as τ_{res} is varied; oppositely, there are not ignition points because the lower tangent is not reached. Moreover, in Fig. 3.11c we notice that a lower nonzero branch is present, corresponding to γ_1.
If the minimum loss-line coincides with the lower tangent, the orange line in Fig. 3.10, the isola and the lower branch just touch as shown in Fig. 3.12.
If the loss line lie below the lower tangent, i.e.

$$4\gamma_0(1-2\gamma_0) > 4/\tau_2, \tag{3.53}$$

then we have the "mushroom" diagram which is illustrated in Fig.3.11d. The isola has now merged with the lower branch to give the "mushroom"

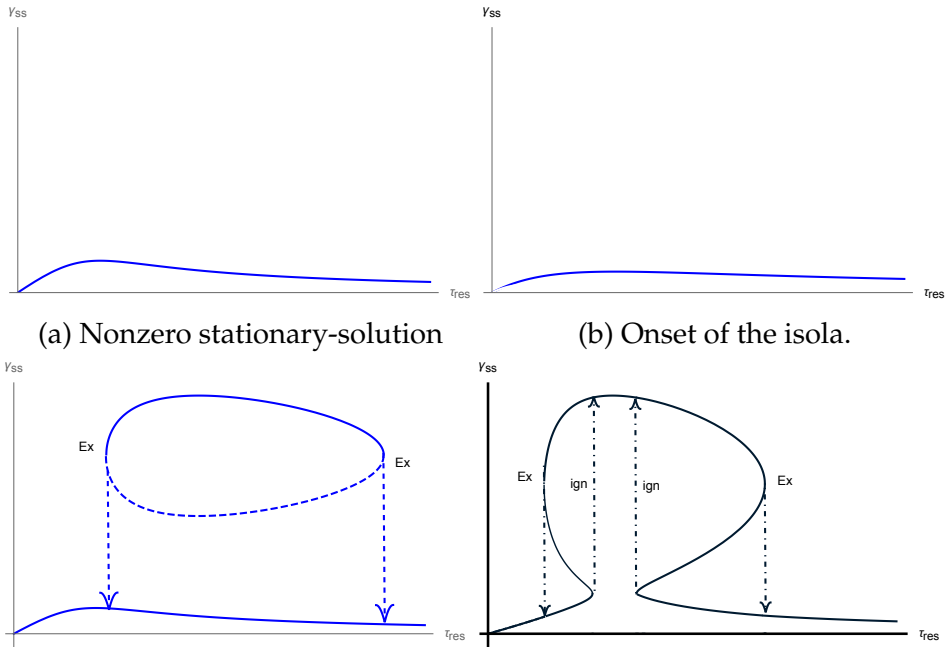

(a) Nonzero stationary-solution

(b) Onset of the isola.

(c) The isola

(d) The mushroom

Figure 3.11: $\gamma_{ss} - \tau_{res}$ diagrams

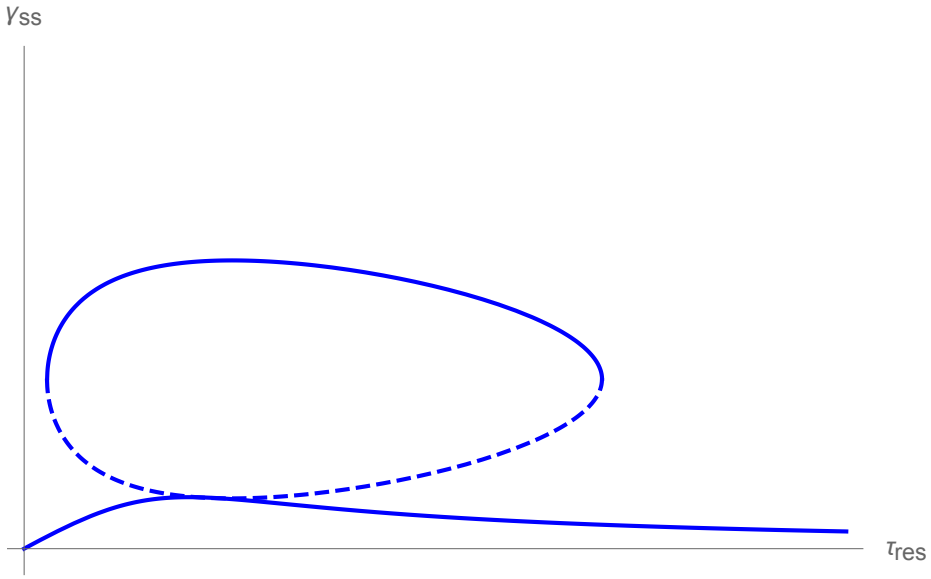

Figure 3.12: The isola touches the lower branch.

characteristic shape. There are two ignition points as well as two extinctions point and two regions over which multistability occurs. In between this regions there is an interval of residence time over which unique solution exists.
The upper range of γ_{ss} is accesible to the system (it existed but could not be reached for the isola).
Manipulating the residence time and the inlet concentration of B in order to obtain a stationary state extent of conversion at the top of the mushroom (which corresponds to a line flatter than the lower tangent in Fig. 3.10 and diagrams in Fig. 3.11d-3.12), a reduction of γ_0 will make the mushroom change to the isola. In this way, the upper side of the isola, which represents stable solutions, can be reached.
As k_2 tends to zero ($\tau_2 \to \infty$) the mushroom streches itself covering infinite residence times.
For large inflow concentrations of B ($\gamma_0 \geq 1/8$), the tangents to the production curve merge and then disappear. Only unique solution are possible with their maximum stationary state conversion for $\tau_2 = \tau_{res}$.
Therefore, for cubic autocatalysis we observe a dramatic change of behaviour if the catalyst is allowed to decay. This instability may be the result of further chemical reaction either due to poisoning or to some physical degradation.

Chapter 4

The Integrin Model

In this chapter, a model describing the biological scheme outlined in the Introduction 1.2 is presented. Integrins are introduced as a two-state diffusing system, where the switching within the states is modulated by the activator and the inhibitor. The central purpose is to mimic the PIP_2 activation pathway and translate it into the mathematical minimal framework. Firstly, the chemical reactions between the integrin receptors, their activator and a controller variable are introduced. Then, the employing of the law of mass action (see Appendix A), will allow for a formulation of a reaction-diffusion model for these three species.
Thereon, once the model has been elaborated we pursue our study using the techniques of dynamical systems. At the end, we will find an exact stationary solution of the model, i.e. the inhibitor and activator profile concentrations in the cellular membrane.
The strategies adopted for seeking the solutions are somehow similiar to those used by Hale, Peletier and Troy for the one-dimensional Gray-Scott model for cubic autocatalysis [5]. However, in this particular model nonlinearity is given by exponential terms so that the handling is challenging. The mathematical methods adopted are similar to those used in [13] and [5], while the construction of this very model can be found in [2].

4.1 Construction of the model

Following the $PIP_2(4,5)$ activation pathway a local increase of the concentration of this component in the membrane leads to integrins recruitment

and consequently to the production of more $PIP_2(4,5)$ itself, consequently starting a positive feedback loop. As pointed out in Chapter 2, these loops mechanisms are very common in biology. In the present case, it is the inhibitor that prevent this feedback production from diverging. In what follows an integrin is a two-states system which can be either:

- Inactive
- Active

Let n_f and n_l be respectively the fraction of free non activated integrins and the fraction of activated/bounded to the ligand integrins. In standard two-variable models, n_l is a given function of u and v and enters as a parameter in the model. Here, in marked contrast, n_l is a dynamic variable adjusting itself to u and v.
In order to keep the problem amenable to analysis, integrins are considered able to diffuse if not activated while they diffuse no longer if they are activated. Actually, these trans-membrane receptors do diffuse over the membrane in the activated bounded to the ligand state as well, but as their diffusion coefficient would be very small, it is neglected for the sake of simplicity.

Besides integrins, the main ingredient of the present model is the activator/inhibitor. Let u be the profile concentration of the activator ($PIP_2(4,5)$) and v be the inhibitor which controls and regulates the production of u by binding to the receptors. An increase of u make integrins to change their conformation in a way that boosts their affinity for the extra cellular ligand. We will assume in what follows that all activated receptors are bound to their ligand. This might not be true generally speaking. In fact, the integrin in the unfold configuration may not necessarily be bounded to the extracellular ligand. In Chapter 5 we add the intermediate state (activated but not bounded) and we modify the system of equations to include it. In that case, we deal with a three-state system.
Beside extracellular ligands integrins can also reversibly bind to a controller protein v representing a kinase, Fig. 4.1. Its presence is required to control the positive feedback loop. The kinase v plays the role of what is called the inhibitor in the language of the dynamical systems. This ligated integrin, a complex that we indicate by "integrin $\diamond$ v", produces u. Production of u favours further integrin activation, favoring the feedback.

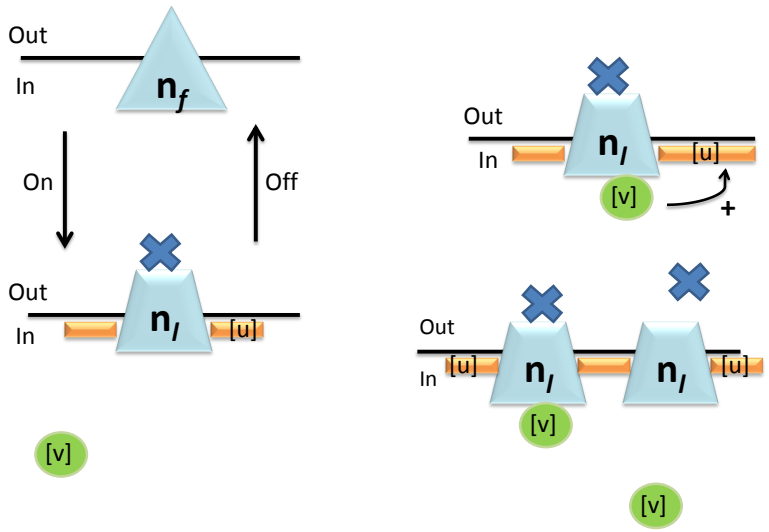

Figure 4.1: Schematic representation of the model. In the left integrin receptors have two conformational states. Inactivated integrins are represented by the regular triangle and activated ones by a triangle with top cut off.ate Changing membrane composition with increasing u as indicated by the color code of the bar drives integrin receptors from their inactivated state to their activated state where they are immobilized by ligation to an extracellular ligand represented by the blue cross. On the right, activated integrins bind reersibly a controller protein represented by a green circle with the symbol [v] forming the complex "integrin $\diamond$ v". The complex "integrin $\diamond$ v" synthetisizes u favoring the activated phase by a feedback loop. This is represented by an arrow and a $+$ sign linking the symbol [u] in the orange bar.

Summarizing, three fundamental players are taken into account in the system:

- Integrins in two conformational states
- Activator ($PIP_2(4,5)$)

- Inhibitor (kinase)

A simplest generic system of reaction-diffusion kind for the activator u and inhibitor v takes the form

$$\begin{cases} \partial_t u = D_u u_{xx} + f(u, v, n_l) \\ \partial_t v = D_v v_{xx} + g(u, v, n_l), \end{cases} \tag{4.1}$$

where $u = u(x,t)$, $v = (x,t)$ and $n_l = n_l(x,t)$ are functions of the space and time coordinates representing the profile concentration of $\mathrm{PIP}_2(4,5)$, kinase and activated integrins respectevely. In general f and g, whose functional form will be given later (see (4.17)), are non linear functions depending on the parameters of the system. Here, n_l depends of dynamic of the system and it adjusts to u or v. To understand the the dynamics of integrins it will be useful to consider their equation of motion. This equation has a diffusive term for free integrins and a kinetic term between the two states, viz.

$$\begin{cases} \partial_t n_f = D_n n_f - k_\uparrow(u) n_f + k_\downarrow(u) n_l \\ \partial_t n_l = k_\uparrow(u) n_f - k_\downarrow(u) n_l, \end{cases} \tag{4.2}$$

where $k_\uparrow$ and $k_\downarrow$ are respectively the on and off rate constants between the two states. These rate constants depend on the activator u, since an increase of u favours the activated state. A convenient choice is to take:

$$k_\uparrow / k_\downarrow \propto \exp(\beta u), \tag{4.3}$$

where β (not to be confused with the thermodynamic $\beta = 1/k_b T$) is some positive constant which has nothing to do with temperature.
The constant β follows from shifts in integrins chemical potentials between the two conformational states finally influencing the relative populations of these two states.
The choice of the exponential behaviour in (4.3) is suggested by analogies with known thermodynamic principles for proteins. This ansatz is also consistent with the Bell's law generally assumed to describe the life time of a bond subjected to a force [3].
As a result, for sufficiently larges u's, $k_\uparrow(u) > k_\downarrow$. Therefore, an increase of u favours the fractional population of activated integrins at the expense of inactivated ones.

In the following diffusion will be crucial. Assuming fixed boundary conditions for n_l and n_f, we find that a stationary solution of (4.2) is obtained for $n_f =$ constant

$$n_l = \frac{k_\uparrow(u)}{k_\downarrow} n_f \tag{4.4}$$

which holds for long times if u is allowed to vary in time and space. The next step is to find the particular form of the functions f and g. Because of the feedback, u is produced at a rate proportional to the complex $n_l \diamond v$ and it is at the same time degraded at a rate proportional to u

$$f(u, v, n_l) \propto -bu + vn_l, \tag{4.5}$$

where b gives characteristic time scale. If the equilibrium between the complex $n_l \diamond v$ is sufficiently fast then the dimensional reduction integrin $\diamond$ $v \propto vn_l$ gives the desired result, since v increases the rate of production of u.
The chemical reactions involving the controller v and the receptors are:

$$n_l + v \underset{\mathrm{k}_-}{\overset{\mathrm{k}_+}{\rightleftarrows}} v \diamond n_l, \tag{4.6}$$

$$\ldots \xrightarrow{1/\tau} n_l + \emptyset, \tag{4.7}$$

where $\emptyset$ represents inert molecules, while the dots represent some other intermediate states that we shall neglect so that we are left with only one effective state. The last step in this equation is decisive for the model. Indeed, it corresponds to a regulation of the complex where a covalent modification of v leads to its irreversible disassembling of the complex $v \diamond n_l$. For the sake of simplicity, it is assumed that in the last step in the reactions, i.e. (4.7), the binding rate is much larger than the unbinding rate so that the reverse reaction can be neglected.
In general one can assume the stationary approximation to hold

$$\frac{dv \diamond n_l}{dt} = 0. \tag{4.8}$$

Substituting Eq. (4.8) in the reactions (4.7) we find

$$v \diamond n_l = \frac{k_+}{k_- + 1/\tau} v n_l. \tag{4.9}$$

Meanwhile considering the overall reaction

$$n_l + v \xrightarrow{1/\tau} n_l + \emptyset, \tag{4.10}$$

we notice that in the equation of motion of v a term coupling u to v appears, namely $(1/\tau)vn_l$. Thus, u is a negative feedback on v since n_l increases with u and v decreases because of the minus sign in the front of the term. Moreover, the controller variable v is produced at a certain rate in order to compensate its degradation occurring at a rate $-1/\tau vn_l$. Assuming thus that the inhibitor v is in equilibrium with a reservoir concentration v_c we find

$$g(u, v, n_l) = hv_c - hv - vn_l. \tag{4.11}$$

Let us put $\tau = 1$ as it sets time reference and scale u and v obtaining:

$$\begin{cases} \partial_t u = D_u u_{xx} + \frac{1}{\epsilon}\left(-bu + vn_l\right) \\ \partial_t v = D_v v_{xx} + h(v_c - v) - vn_l \end{cases} \tag{4.12}$$

where has been imposed

$$\frac{1}{\epsilon'} = \frac{k_+}{k_- + 1/\tau}\frac{\tau}{\epsilon}, \tag{4.13}$$

before dropping the prime. Due to diffusion and on long time scales the homogeneous distribution of integrins over the membrane can be postulated. Therefore we have:

$$\partial_t n_l = k_\uparrow(u) n_f - k_\downarrow(u) n_l = 0, \tag{4.14}$$

with $n_f = \text{cst}$.
Using (4.3) and (4.4)

$$n_l(u) \sim e^u, \tag{4.15}$$

with $\beta = 1$ for simplicity. Imposing

$$B = \frac{b}{\epsilon}, \quad A = hv_c \tag{4.16}$$

We obtain the following system:

$$\begin{cases} \partial_t u = D_u \dfrac{\partial^2 u}{\partial x^2} + ve^u - Bu \\ \partial_t v = D_v \dfrac{\partial^2 v}{\partial x^2} - ve^u + A\left(1 - v\right), \end{cases} \tag{4.17}$$

which is a highly nonlinear system of differential equations. Here also the diffusion term is present because both inhibitor and reactor can spread over the membrane. This system is found to be extremely outside equilibrium and it cannot be derived from a variational principle such as the minimization of a functional. It is precisely this feature that permits us to find stationary localized structures as spike waves where u and v deviate strongly from their homogeneous value in a localized domain of space, see figures 4.6 and 4.7. From now on, we will focus on the system (4.17) showing how we can obtain an exact solution of this system for a particular choice of the parameters.

4.2 Geometrical properties

A useful graphical method for investigating the qualitative behavior of solutions of a system is the study of nullclines. As the system may be generally written as

$$\partial_t u = f(u, v) \tag{4.18}$$

$$\partial_t v = g(u, v), \tag{4.19}$$

where diffusion has been neglected, the nullclines are founded imposing $f(u, v) = 0 = g(u, v)$, being tthe curves having the same gradient. Hence, they are given by the set of equations

$$ve^u = Bu, \tag{4.20}$$

$$ve^u = A(1 - v). \tag{4.21}$$

Fixed points in the homogeneous state are given by isoclines intersections which they are found to lie on the line of equation $Bu = A(1 - v)$. We are able to plot both nullclines curves and the line where fixed points lie numerically. Depending on the parameters in the (A,B) plane, two kinds of scenarii are possible: one fixed point see 4.2b and 4.2b or three fixed points, see 4.3.

In what follows, we work in the monostable regime i.e. one fixed stable point i.e. the situation present in 4.2a. In figure 4.2b we have instead one fixed non-stable point where the solution oscillates.

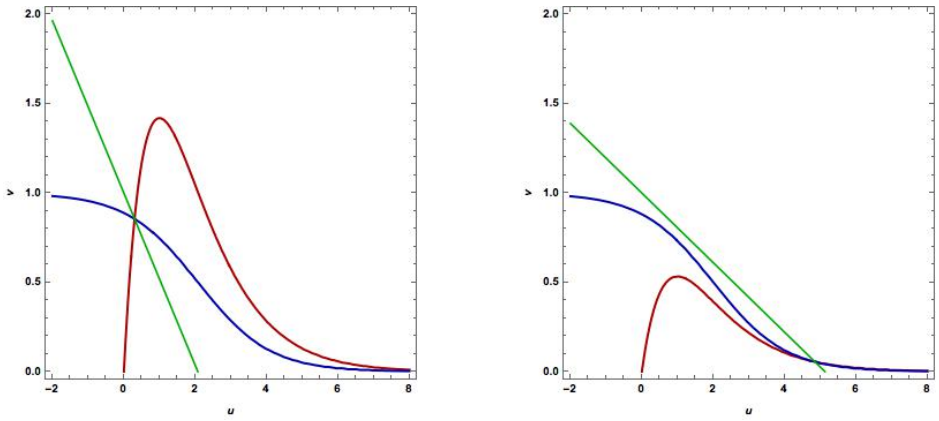

(a) $A > B \quad (B = 4, A = 2)$ (b) $A < B \quad (B = 1, A = 7)$

Figure 4.2: Nullclines with one fixed point

The equations (4.17) can be simplified by introducing a dimensionless constant and performing a scaling:

$$\tilde{x} = \frac{1}{\sqrt{D_v}} x, \quad w = \frac{D_u}{D_v} \tag{4.22}$$

we obtain then

$$\begin{cases} \partial_t u = w \dfrac{\partial^2 u}{\partial x^2} + v e^u - Bu \\ \partial_t v = \dfrac{\partial^2 v}{\partial x^2} - v e^u + A\,(1 - v) \end{cases} \tag{4.23}$$

where the tildes have been dropped. In the case of stationary solutions the system of equations becomes

$$\begin{cases} 0 = w \dfrac{\partial^2 u}{\partial x^2} + v e^u - Bu \\ 0 = \dfrac{\partial^2 v}{\partial x^2} - v e^u + A\,(1 - v) \end{cases} \tag{4.24}$$

Eq.ns (4.24) are highly nonlinear so that it is quite far from obvious evaluate an analytical solution. We will demonstrate in the next section the existence of an exact non trivial solution

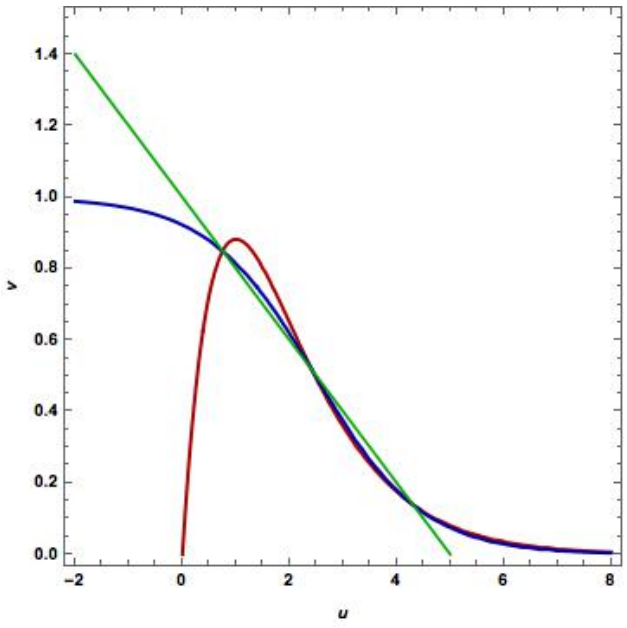

Figure 4.3: $A > B \quad (B = 2.4, A = 12)$
Three fixed points

4.3 Exact solutions

The main purpose of this section is to find exact solutions consisting of a family of homoclinic orbits, as seen in [5]. These orbits are symmetrical with respect to x, so they satisfy

$$u(x) = u(-x) \quad \text{and} \quad v(x) = v(-x), \tag{4.25}$$

$$u'(0) = 0 \quad \text{and} \quad v(0) = 0; \tag{4.26}$$

and they describe localized solutions approaching the only fixed point value as $|x| \to \infty$. Exact solutions in the form of homoclinic orbits can be found only for very particular values of parameters that is:

$$B = Aw \quad \text{and} \quad w \ll 1 \tag{4.27}$$

So that the exact solution's domain is very small. Introducing the auxiliary function P defined as

$$P = wu + v - 1, \tag{4.28}$$

deriving both members two times,

$$P'' = wu'' + v''; \tag{4.29}$$

and adding member by member (4.24), we obtain

$$\begin{cases} P'' = wu'' + v'' = Bu - A(1 - v) \\ P = wu + v - 1 \end{cases} \tag{4.30}$$

Taking A times the second equation in (4.30) and subtracting from the first one in (4.30) one obtains the following system with initial value problem

$$\begin{cases} P'' - AP = (B - Aw)u \\ P(0) = wu(0) + v(0) - 1 \\ P'(0) = 0 \end{cases} \tag{4.31}$$

For the special case:

$$B = Aw, \tag{4.32}$$

problem (4.31) reduces to:

$$\begin{cases} P'' - AP = 0 \\ P(0) = wu(0) + v(0) - 1 \\ P'(0) = 0 \end{cases} \tag{4.33}$$

Thus, if $P(0) = 0$ and $P'(0) = 0$ the solution of the differential equation is of the kind:

$$P(x) = c_1 e^{\sqrt{A}x} + c_2 e^{-\sqrt{A}x} \tag{4.34}$$

then cauchy's problems give

$$c_1 = -c_2 \quad \text{and} \quad c_1 = c_2 \tag{4.35}$$

leading to

$$P(x) = 0 \qquad \forall x \in \mathbb{R} \tag{4.36}$$

and

$$wu(x) + v(x) - 1 = 0 \quad \forall x \geq 0 \tag{4.37}$$

We can consequently eliminate v from the first equation in (4.24) giving,

$$u'' = \frac{1}{w}\left[(wu - 1)e^u + Bu\right] \tag{4.38}$$

4.4 A mechanical analogy

If we think of u and x as position and time of a unitary mass particle respectively, then Eq. (4.38) represents the total force acting on this system. We can therefore compute the potential which constrains the particle. Integrating and changing the sign of (4.38) we have:

$$V(u) = \frac{1}{w}\left[e^u - w(u-1)e^u - B\frac{u^2}{2}\right]. \tag{4.39}$$

Multiplying both members in (4.38) by u' it is soon found:

$$wu''u' = u'\left[(wu-1)e^u + Bu\right] \tag{4.40}$$

$$\left(\frac{wu'^2}{2}\right)' = u'\left[(wu-1)e^u + Bu\right], \tag{4.41}$$

so that integrating once both members with respect to x yields

$$\frac{u'^2}{2} + V(u) = cost.te = \mu, \tag{4.42}$$

which is nothing more than the conservation of mechanical energy.
In order to have a bounded orbit, we may choose the constant μ as being equal to the value of the potential's maximum (which occurs for u zero in 4.4). Considering the case in which the inhibitor has a much larger diffusion length than the one of the activator

$$D_v \ll D_u \implies w \ll 1, \tag{4.43}$$

then the potential has the form shown in Fig. 4.4.

As we are looking for homoclinic solutions, in the activator case for this condition is satisfied by the following boundary conditions

$$\lim_{x\to\infty}\big(u(x), u'(x)\big) = \big(u_h, 0\big), \tag{4.44}$$

where u_h is the fixed point. In order to evaluate the constant μ which appears in the conservation energy equation (4.42), we take the limits at

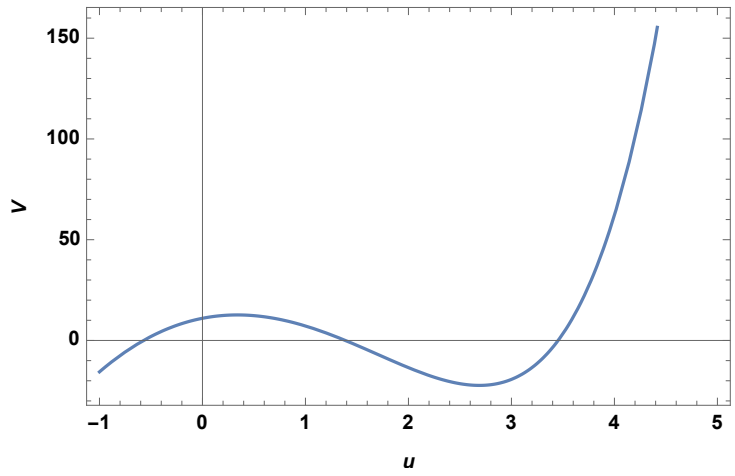

Figure 4.4: Potential function ($w = 0.1$ and $B = 4$)

infinity. Staying in the case $B = 4$ and $w = 0.1$, we obtain the following values

$$\lim_{x\to\infty} V(u) = \mu \approx 12.67 \tag{4.45}$$
$$(u_h, v_h) \approx (0.34, 0.96)$$

where the calculation has been evaluated using numerical techniques. Plotting the phase portrait curves i.e. the plane (u, u') we find

In figure 4.5 we can immediately tell that the solutions have the expected qualitative properties. In fact, the closed orbit tells us that the inhibitor concentration profile function derivative u' is zero for $x \to -\infty$; then, it grows for increasing x's since it reaches a maximum; nextly, it decreases until vanishing at $x = 0$; then it becomes negative until it reaches a minimum and then it grows again reaching zero for $x = +\infty$.
Equivalently, the profile concentration u vanishes for $x = \pm\infty$ and exhibits a maximum at the origin i.e. for $x = 0$. In order to seek exact solution of the problem we come back to the energy conservation equation (4.42). Isolating u' and performing the separation of the variables yields

$$\frac{du/\sqrt{2}}{\sqrt{\mu - V(u)}} = dx. \tag{4.46}$$

This is a separable variable differential equation, but unfortunately, for the reason that it does not admit a primitive function, it is required to

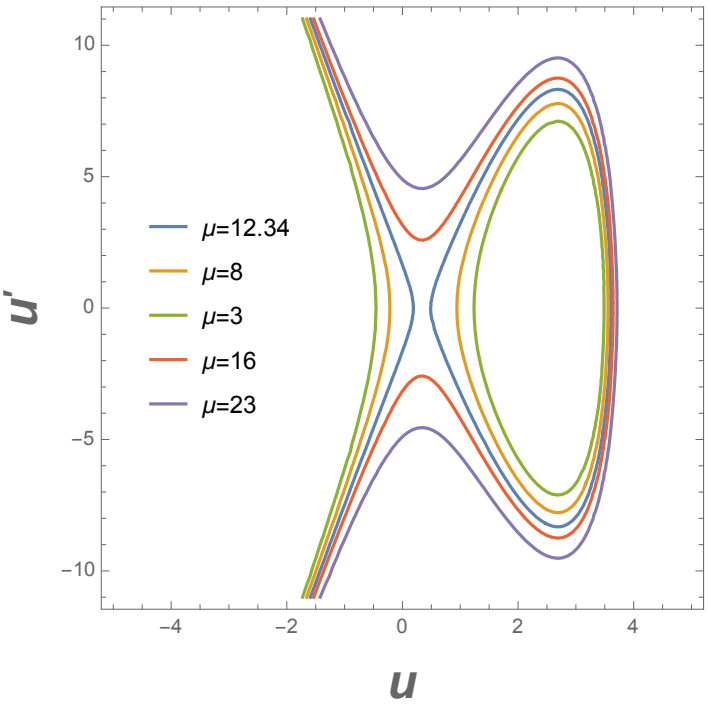

Figure 4.5: The phase plane

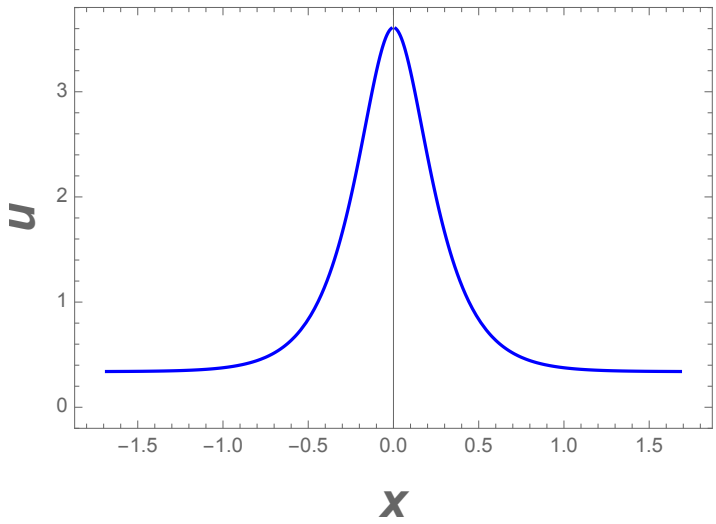

Figure 4.6: Exact solution reactor u

compute the solution numerically. As we seek a bounded solution, we recall the potential form in 4.4 and we choose our constant μ to have the value of the maximum of the potential. In this way we may be able to plot the exact solution for u when it is varying in the range between the point relative of the first maximum of the potential and the maximum point for which the potential reaches again the maximum value i.e.

$$\mu = 12.67, \tag{4.47}$$

which occurs for $u = 0.339$. Integrating numerically both members in (4.46) and recalling the relation between u and v, $v = 1 - wu$ we can plot now both solutions as shown in figures 4.6 and 4.7

4.5 Conclusions

As expected, in figures 4.6 and 4.7 the activator and the inhibitor concentrations exhibit respectively a maximum and a minimum in correspondence of the origin of coordinates; in other words as the concentration of the activator PIP_2 raises inside a region in the cell's membrane, say the origin, the system responds with a consequent decrease of controller's concentration; being a source of PIP_2 production, a decrease of the inhibitor

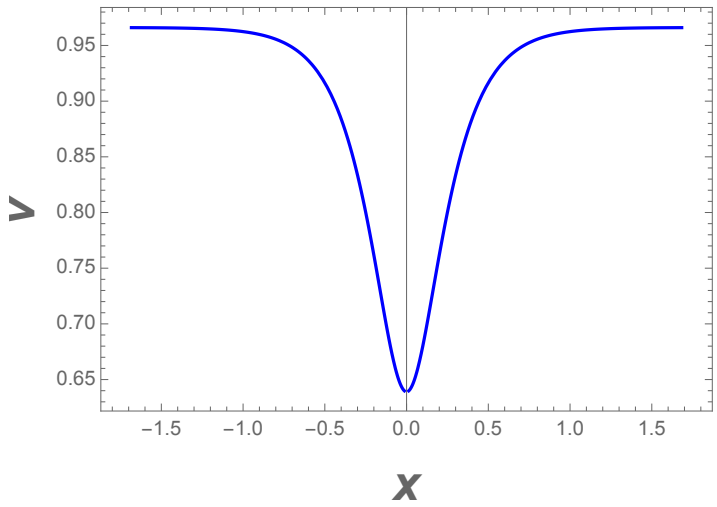

Figure 4.7: Exact solution inhibitor v

kinase will finally lead to a decrease of the activator, limiting and controlling the grows of PIP_2.
Another remarkable feature illustrated in 4.6 and 4.7 is that the variation in concentrations have approximately the same scale while usually approximate solutions vary in totally opposites regimes. In terms of receptors, the model predicts a peak of activated integrins n_l in the neighbourhood of the origin as the activator has a spike in that zone.
Starting from an initial condition in which these receptors are uniformly spread all over the membrane, when a signal is delivered to the cell a raise the activator concentration occurs, leading to a local increase of activated integrins in this area. Then, a stationary state outside equilibrium represented by a pulse and kink type solution is allowed.
In this work, parameters such as the diffusion lengths had been properly chosen in order to have a particular potential form in 4.4. However, this form can qualitatively occur for other values of the diffusion lengths so that we can actually make vary this parameter along a certain interval. In this range we can always find an exact solution of the same kind.

Chapter 5

Integrin Dynamics

In this final chapter, in order to see what the model predicts in terms of integrin dynamics we perform a simulation. Having showed in Chapter 4 that the integrin model allows spike solution for the activator u, in what follows we investigate integrin arrangement when a very simple function for u is given. In other words, we study solutions of the partial differential equation (5.2) describing integrin motion when the activator enters as a boxcar function in space and it stays as such for all times.

5.1 Basic configuration setup

To keep the problem amenable to analysis, the test is performed in a limited planar zone of the celllular surface, a squared shaped region. Inside this square, the activator u is distributed as the shaded blue part of Fig. 5.1. Considering an initial situation where integrins in whichever state (free and ligated) are homogeneously distributed, when the disk annulus is filled with the activator, free integrins placed inside the annulus region should activate soon and consequently paralyze, while the ones that are located in the non activated zones, outside the disk annulus and in the bullseye region, are actually free to diffuse.
As time goes by, freely moving integrins may fall in the activated region as well, if one waits enough time.

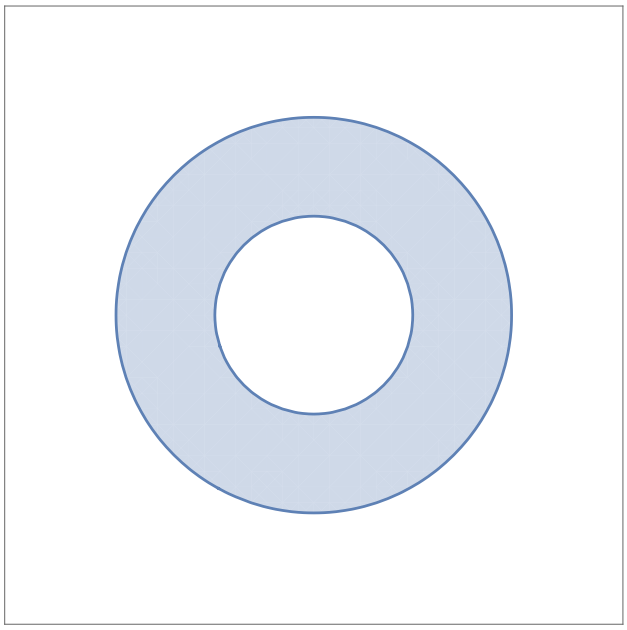

Figure 5.1: The plane portion of the cell. The activated zone is the blu annulus, while the rest (the white circle inside the annulus the so called bullseye and the white zone outside the annulus) is free from u.

5.2 System of PDE

The system of partial differential equation for integrin dynamics is

$$\partial_t n_f = D_n \Delta n_f - k_\uparrow n_f + k_\downarrow n_l; \tag{5.1}$$

$$\partial_t n_l = k_\uparrow n_f - k_\downarrow, \tag{5.2}$$

where $k_\uparrow$ and $k_\downarrow$ are the on and off rate constants between the two integrin states. This is a system of PDE of the second order involving two unknown variables, i.e. $n_f(x,t)$ and $n_l(x,t)$. Remarkedly, the diffusion term is present only in the first equation (Eq. (5.2)) of the system as only free integrin are able to diffuse while ligated integrins are stacked into the membrane and cannot move. We assume then the following relationships for the rates

$$k_\uparrow = K_+ \exp\left(\frac{\beta u}{2}\right); \tag{5.3}$$

$$k_\downarrow = K_- \exp\left(-\frac{\beta u}{2}\right). \tag{5.4}$$

In the first place we have to specify the boundary conditions. Let us consider an initial situation when where both free and ligated integrins are homogeneously distributed all over the square. Then, after some time, say 10 seconds, we switch on the annulus region.
Because of the manifest symmetry of the problem, the number of dimension can be reduced from two to one. In fact, passing from cartesian to polar cordinates we have $(x,y) \to (r,\theta)$, r is the radius from the origin and θ is the polar angle. In this sytem of coordinates is evident that the polar angle θ is a cyclic coordinate. That being said, we can actually plot the step function for the activator as a typical boxcar function in one spatial dimension r, Fig. 5.2. As one can notice in Fig. 5.2, a suitably smooth version of the mathematical boxcar function has been adopted. In this way, one can serenely insert $c(r)$ as an input function in a computational knowledge engine without worrying about any retaliation. The trick to have a smooth version of the boxcar function is the following selection of combination of hyperbolic tangents

$$c(r) = \tanh\left(\frac{r-a}{\delta}\right) - \tanh\left(\frac{r-b}{\delta}\right), \tag{5.5}$$

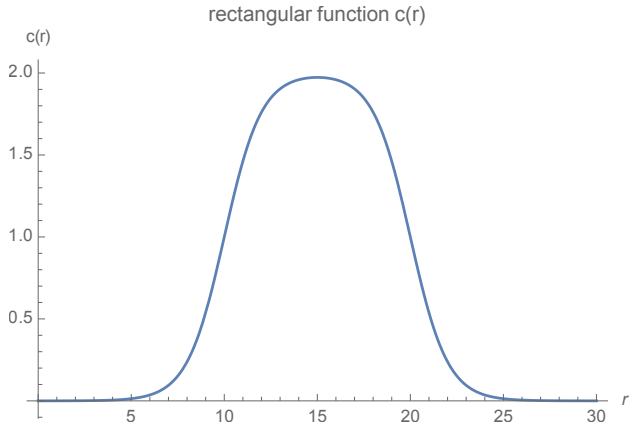

Figure 5.2:
Smooth boxcar function $c(r)$ in one dimension

where a and b are are the extrema of the interval over which the function is not zero, while δ regulates the steepness. The bigger is δ the smoother becomes the boxcar function, while the smaller is δ the more it approaches to a boxcar mathematical function. As the problem lowered down to one spatial dimension, we can introduce the time straightforwardly in order to make our smooth boxcar function dependent on both time and space. We may suitably choose our two dimensional boxcar function for the activator as

$$u(t,r) = \left[1 + \tanh\left(\frac{1}{2}(t - t_0)\right)\right] c(r), \tag{5.6}$$

where t_0 is the starting time of the simulation. Notice how the choosen boxcar function $u(r,t)$ is smooth in both radial and time directions. This is due to the introduction of the product of the two hyperbolic tangents. The $u(r,t)$ activator function, as we can see in Fig.5.3, is zero until about 10; then it rises in the boxcar shape for $t \simeq 10$. Taking a picture at any time t with $t > 10$ will yield the smooth boxcar function in one dimension of Fig. 5.2.

5.3 PDE solutions for integrins

As we deal with a non-linear partial differential equation we cannot even hope to find a an analytical solution, we must make the computer eval-

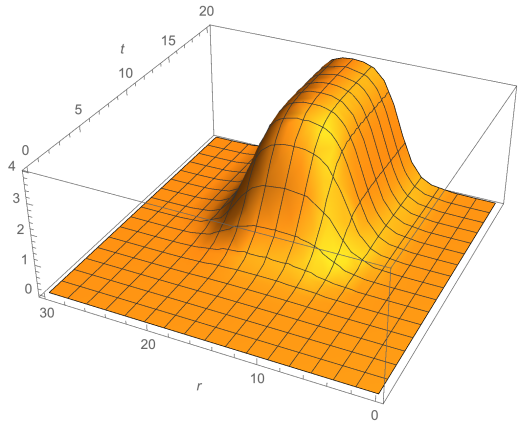

Figure 5.3: The 2-dimensional boxcar function activator $u(r,t)$.

uate a numerical solution for us. First of all, we must set the boundary conditions

$$\partial_r n_f(r=0,t)=0 \tag{5.7}$$

$$\partial_r n_f(r=r_{\max},t)=0. \tag{5.8}$$

The set of eq.ns (5.8) is the so called zero flux boundary conditions.

In order to make the simulation work properly we must assign a diffusion coefficient to ligated integrins as well. Assigning a three order magnitude smaller coefficient to bounded integrins $D_{\text{free}}=10^3 D_l$, we find the solutions shown in Fig. 5.4 - 5.5. As expected, both free integrins and ligated integrin solutions $n_l(r,t)$ and $n_f(r,t)$ are almost symmetrical with respect to the center of the boxcar function, i.e., reflection symmetry with respect to the $r=15$ plane. The asymmetry is related to the different density of integrins in the bullseye region and in the region outside the annulus. In fact, as we have assumed an homogeneous distribution all over the square, we have clearly more integrins outside the annulus region than in the bullseye region, the latter being smaller. For this reason we have

$$n_f(r^\star,t)\leq n_f(r^\dagger,t); \tag{5.9}$$

$$n_l(r^\star,t)\leq n_l(r^\dagger,t) \tag{5.10}$$

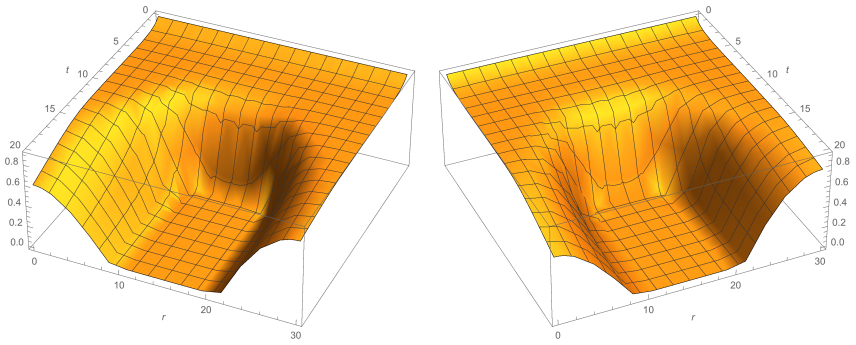

(a) From the left-side (b) From the right-side

Figure 5.4: Free integrins solution of PDE $n_f(r,t)$ plotted in three dimension from different perspectives

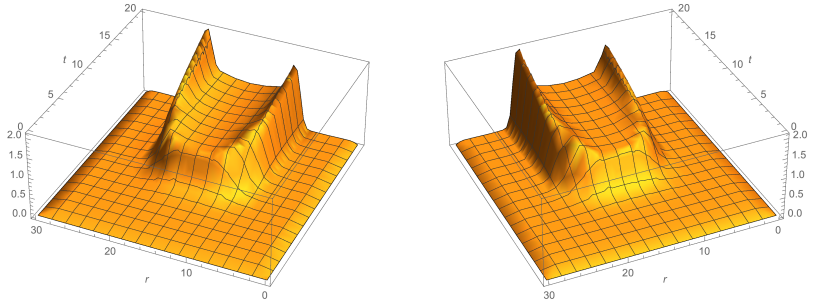

(a) From the left-side (b) From the right-side

Figure 5.5: Free integrins solution of PDE $n_l(r,t)$ plotted in 3D

where $r^\star \in I_\star$ and $r^\dagger \in I_\dagger$ with

$$I_\star = \{r|0 < r < 15\}$$

$$I_\dagger = \{r|15 < r < 30\}.$$

Moreover, another striking feature is the appereance of the two spikes in correspondence of the borders of the activated region giving as a result the batman head shape of Fig. 5.5. This occurs because as far as we know, free integrins are likely to bound as soon as possible so that they don't wait to get too far inside the activated region to activate themselves. We notice in Fig. 5.5 that for $t \sim 10$, the profile of the ligated integrin density $n_l(r, t = 10)$ is very similiar to the boxcar function, while after that, the spikes in the borders become higher and higher as time goes by. This is because around $t = 10$ all free integrins inside the activated zone become ligated but after, for $t > 10$, more free integrins are coming both from the unactivated zones inside and outside the annulus. As they come from the unactivated zones, free integrins are more likely to bind as soon as they touch the activator, giving rise to the big spikes and accumulating in the borders.

5.4 Different rates dependencies solutions

In the last section has been assumed a dependence on the activator u for both rates Eq.(5.4), but as only the quotient K_+/K_- really counts it is up to us to choose the u law provided that the quotient stays in the usual form

$$\frac{k_\uparrow}{k_\downarrow} = \frac{K_+}{K_-}\exp(\beta u). \tag{5.11}$$

We may try simulations for both cases in which one of the two rates is a constant and make a comparison in addition to the one considered in the previous section i.e.

A	$k_\uparrow(u) = K_+\exp(\beta u/2)$	and	$k_\downarrow(u) = K_-\exp(-\beta u/2)$
B	$k_\uparrow(u) = K_+$	and	$k_\downarrow(u) = K_-\exp(-\beta u)$
C	$k_\uparrow(u) = K_+\exp(\beta u)$	and	$k_\downarrow(u) = K_-$

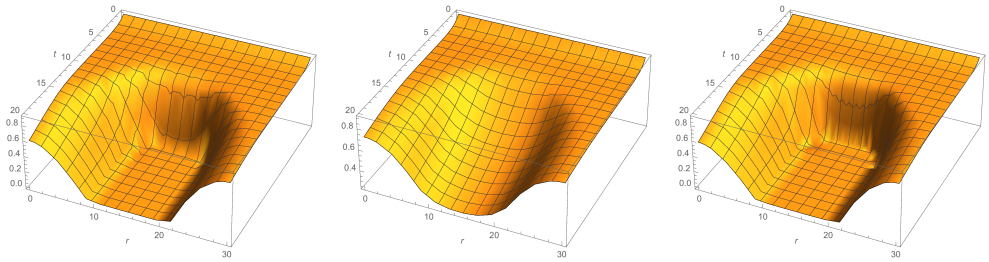

(a) **A** (b) **B** (c) **C**

Figure 5.6: comparison among three different rate choices **A**, **B** and **C** for the free integrins PDE solution $n_f(r,t)$

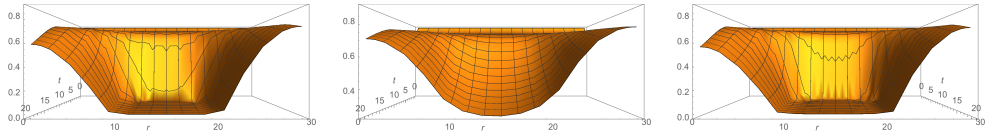

(a) **A** (b) **B** (c) **C**

Figure 5.7: comparison among three different rate choices **A**, **B** and **C** for the free integrins PDE solution $n_f(r,t)$ seen from the front

Plugging in the three different rates **A**, **B** and **C** we find the results shown in Fig.5.6 and Fig. 5.8. The behaviour of the **B** rate shown in Fig.5.7b, Fig. 5.6b and Fig. 5.8b is qualitatively sensibly different than the other two even if all cases show the same beavior for small u. In fact, in **B**, solutions exhibit a smoother change in correspondence to the activated region. What is more, it takes higher overall values in the free integrin solution n_f Fig. 5.7b, and lower overall values in the n_l solution Fig.5.8b, the latter not exhibiting the border spike behavior. The main cause of this striking behavior is the fact that in the case in **B** the activation rate $k_\uparrow$ is constant. As a result in case **B** the activation process alone is not "feeling" any difference when passing in the activated zone because the rate is the same everywhere.
Considering a free integrin in the bullseye region; as it is free to diffuse it can either stay in the bullseye region or, after some time, can enter in the activated zone inside the annulus. In both cases, if one takes into account that integrins can bind and release continously, then, there will be no difference in the probability of activating itself, neither staying all the

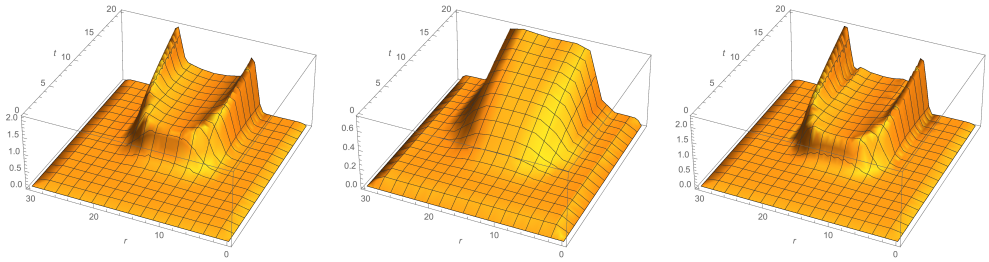

(a) **A** (b) **B** (c) **C**

Figure 5.8: comparison among three different rate choices **A**, **B** and **C** for the ligated integrins PDE numerical solution $n_l(r,t)$

time inside the annulus nor in the bullseye region. One could ask then: why there is any evidence at all of absence of free integrins in the annulus, i.e. for $10 < r < 20$, Fig. 5.6b or any evidence of presence of ligated integrins in the very same zone Fig. 5.8b. Why it is not just flat everywhere? The answer is in the unactivation rate $k_{\downarrow}$ of case **B**; in fact, it depends exponentially on the activator u which depends itself on r. Hence, it is the inactivation rate which decays exponentially in the annulus that justifies the presence of ligated integrins in the very same region (FIg.5.8b) as well as the absence of free integrin in the very same region (Fig.5.6b).
Summarizing, for case **B**, a free integrin in the annulus has a constant probability to bind, then, once bounded it does diffuse, but very slowly (having imposed a very small diffusion coefficient for ligated integrins).
Another scenearium is that, once bounded, the integrin placed in the annulus, can release the ligand break free and move faster, but the probability that this occurs is very small (exponential decay in the rate of release).
On the other hand, suppose we have one ligated integrin inside the annulus but close to the borders: as the integrin moves really slowly towards the unactivated zone it experiences an increase of the probability of unactivating finally reaching (when $u = 0$), the constant and maximum value K_-. This is the reason why the deactivating process takes more time than case **A** and **C**, when integrins escape from the annulus and, as a result ,the borders thereon are smoother. In fact, in both cases **A** and **C** the unactivation rate is bigger

$$K_- \leq K_- \exp(-\beta u/2) \leq K_- \exp(-\beta u). \tag{5.12}$$

It deactivates slower because the rate is the smallest of the three cases.

Moreover, as previously stated, in **B**, we have no more spike borders of ligated integrins n_l (Fig.5.8) as free diffusing integrins will not change the activating rate when crossing the borders. As a result, ligated intergrins escaping the annulus unactivate slower.
On the other hand, comparing the other two rates with each other **A** and **C**, Fig. 5.7a, 5.6a and 5.8a, we do not remark any significant difference. In fact, as it is the activation rate that controls the mechanism, the two cases **A** and **C** have almost the same activation rates but different deactivations. Moreover, the latters are recovered in the limit of small concentrations of the activator

$$k_{\downarrow \mathbf{A}}(u) \xrightarrow{u \to 0} k_{\downarrow \mathbf{C}}(u) \tag{5.13}$$

The biggest difference between these two cases must occur inside the annulus where u, the boxcar function exhibits the maximum, in fact therein we have the greatest discrepancy between the off rates $k_{\downarrow \mathbf{A}}(u)$ and $k_{\downarrow \mathbf{C}}(u)$ i.e.

$$k_{\downarrow \mathbf{A}}(u_{\max}) \simeq 10^{-4} \qquad \text{and} \qquad k_{\downarrow \mathbf{C}}(u_{\max}) \simeq 1. \tag{5.14}$$

However, this descrepancy is well neutralised by the two on rates, i.e.

$$k_{\uparrow \mathbf{A}}(u_{\max}) \simeq 10^{3} \qquad \text{and} \qquad k_{\uparrow \mathbf{C}}(u_{\max}) \simeq 10^{7}. \tag{5.15}$$

As a result, in the region $u_{\max}$ the greatest difference in the off rates is neutralised by the one of the on rates and we do not see any remarkable difference as expected (Fig. 5.6a - 5.6c - 5.8a - 5.8c).

5.5 Three-states integrin model

In what follows, we add a third state for integrins in order to make the model more realistic. As a matter of fact, until now no difference has been made between activated and ligated integrins, and we have used both definitions equivalently. In order to compare the result with the previous case we introduce a limited reservoir of ligands as well.

5.5.1 Finite ligands concentration

Until now, the ligand concentration has not been taken into account, indeed we have dealt with a system with an infinitely big in size reservoir

of ligands. As a result, each time an integrin was found in the upright position then it was considered automatically bounded. This is not often the case. For instance, a leucocyte moving in the blood vessel may bind or not with endotelial cells (the walls), depending on the availability of extracellular ligands. Additionally, if not enough interacting ligands are present a cell may duplicate or not. If these interactions are lost, the cell may become cancerous. These are only few examples that strongly motivate this condition to be taken into account.
A question to be investigated in order to make the model more realistic would be then "how one can modify eq.ns (5.2) to include finite ligands concentration?". In the first place one must intervene in the rates $k(u)$ because as far as we have noticed, they represent the key in the activation process dictating where and how the activation process take place.
First requirement we must consider is that we need the activation process to stop as soon as there are no ligands available. Secondly, the activation process must be directly linked to the availability of ligands in a way that the more ligands are available, the more likely is the activation process.
One may then proceed as follows, first we introduce a finite reservoir of ligands c_{tot} which is composed of free ligands and bound ligands, i.e., using the usual logic for the subscritpts

$$c_{\text{tot}} = c_f + c_l. \tag{5.16}$$

Then we make the rates k depend on the ligands, so that the system (5.2) becomes

$$\begin{cases} \partial_t n_f &= D_n \Delta n_f - k_\uparrow(u, c_f) n_f + k_\downarrow(u, c_f) n_l; \\ \partial_t n_l &= k_\uparrow(u, c_f) n_f - k_\downarrow(u, c_f) n_l. \end{cases} \tag{5.17}$$

where, as described previously, the rates have the following law

$$k_\uparrow(u, c_f) = k(u) c_f; \tag{5.18}$$

$$k_\downarrow(u, c_f) = k(u) c_f (c_{\text{tot}} - c_f). \tag{5.19}$$

In this way the on rate is directly proportional to the free ligands concentration c_f, while the off rate is directly proportional to the bounded ligands concentration. The more ligands are accessible (free), the more will finally bind with integrins; the more ligands are bounded, the more will be re-

leased. The system of equations (5.17) can be written as

$$\begin{cases} \partial_t n_f &= D_n \Delta n_f - k_\uparrow(u) c_{\text{tot}} (c_f / c_{\text{tot}}) n_f + k_\downarrow(u) c_{\text{tot}} \left[1 - (c_f / c_{\text{tot}})\right] n_l; \\ \partial_t n_l &= k_\uparrow(u) c_{\text{tot}} (c_f / c_{\text{tot}}) n_f - k_\downarrow(u) c_{\text{tot}} \left[1 - (c_f / c_{\text{tot}})\right] n_l. \end{cases} \tag{5.20}$$

Remarkedly, when all the ligands are free $c_{\text{tot}} = c_f$ the activation rate is maximum viz.

$$k_\uparrow(u, c_f) = k_\uparrow c_{\text{tot}}, \tag{5.21}$$

then normalizing the total concentration $c_{\text{tot}} \to 1$ we recover exactly the rate of the previous sections, meaning that the avaiability of ligands is again infinite.
On the other hand, the off rate reaches its minimum

$$k_\downarrow(u, c_f) = 0. \tag{5.22}$$

which is reasonable, as no integrins are bounded to no ligand then no ligand can be released; as a result, we have a zero off rate. On the other hand, when all ligands are bounded $c_f = 0$, which yields

$$k_\uparrow(u, c_f) = 0; \tag{5.23}$$

$$k_\downarrow(u, c_f) = k_\downarrow(u) c_{\text{tot}}. \tag{5.24}$$

Equation (5.24) means that the process of activation stops as soon as the ligands avaibility ends, which was the first of our requirements. Again, if imposing $c_{\text{tot}} = 1$ we recover the off rate of the previous sections.

5.5.2 Three-state integrin system equations

Next step to make the system more realistic is to pass from a *two* states system to *three* states, including the case where the integrin is activated (in the upright position) but not bounded, as represented in (B) Fig. 1.1. Summarizing, we now have

- free non activated integrins n_f
- activated non bounded integrins n_a
- activated bounded integrins n_l

we now have to add two more new taxes related to the brand new integrin state, namely $k_{\Uparrow}$ and $k_{\Downarrow}$ representing the bounding and the releasing rate respectively. Schematically, we can represent the rates as follows

$$N_f \underset{k_{\downarrow}(u)}{\overset{k_{\uparrow}(u)}{\rightleftarrows}} N_a + \underset{k_{\Downarrow}}{\overset{k_{\Uparrow}}{\rightleftarrows}} N_l. \tag{5.25}$$

Next, we may modify the equations 5.2 in order to incorporate such new taxes, than using the usual method we obtain a system of three differential equations viz.

$$\begin{cases} \partial_t n_f &= D_n \Delta n_f - k_{\uparrow}(u) n_f + k_{\downarrow}(u) n_a; \\ \partial_t n_a &= (D_n/4)\Delta n_a + k_{\uparrow}(u) n_f - k_{\downarrow}(u) n_a + \\ & \qquad\qquad - k_{\Uparrow}(c_{\text{tot}} - n_l) n_a - k_{\Downarrow} n_l; \\ \partial_t n_l &= k_{\Uparrow}(c_{\text{tot}} - n_l) n_a - k_{\Downarrow} n_l. \end{cases} \tag{5.26}$$

The first equation in (5.26) has not been changed at all (altough n_l is replaced by n_a), the last one in (5.26) has not either but for the rates, and an equation (the one in the middle in system (5.26)) has been added to the system (5.26). The equation of motion for acrtivated integrins contains a diffusion term, but with a smaller diffusion coefficient. This is because not bounded activated integrins are allowed to diffuse but not as much as the ones that are free. Hence, the activated not bounded integrin is the intermediate state between the ligated one and the free state; in fact, in the equation of motion for this intermediate state, all the rates of the system are involved.
Notice how only the activating rates concerning the trasformation between the fold and the unfold state depend on the activator u, and not on the concentration of the ligands.
In the middle and last equations (5.26), the substitution $c_l = n_l$ has been made, in fact the number of ligands bounded is equal to the number of integrins bounded.
On the other hand, the rates $k_{\uparrow}$ and $k_{\downarrow}$ concerning the switching between the upright not ligated state and the upright ligated state do depend on the ligand concentration as it should be. In fact, the switch from the bent configuration to the intermediate upright position should be independent from the ligands as well as the rate of bounding should be independent on

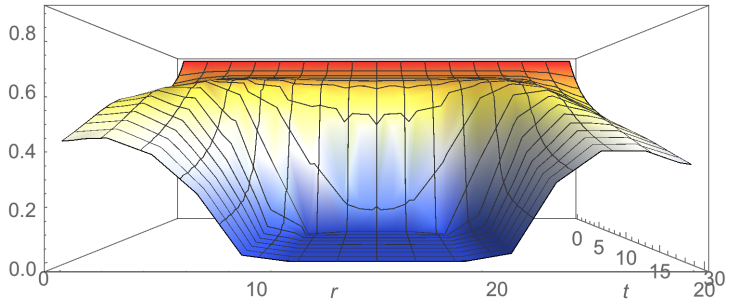

(a) $n_f(r,t)$

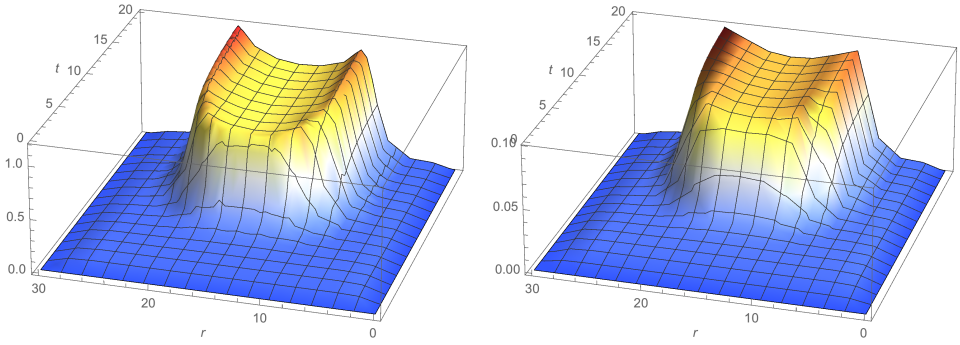

(b) $n_a(r,t)$ (c) $n_l(r,t)$

Figure 5.9: Solutions of the system (5.26)

the activator u. Moreover, the stop requirement is satisfied when all ligands are bounded, $c_f = c_{\text{tot}}$ and we have the stop in bounding, $k_{\Uparrow}(c_{\text{tot}} - c_{\text{tot}}) = 0$; oppositely, when the ligands are all available, the bounding rate reaches its maximum $k_{\Uparrow} c_{\text{tot}}$. Solutions can be found numerically imposing the following values for the parameters: $c_{\text{tot}} = 1$, $k_{\Downarrow} = 1$, $k_{\Uparrow} = 1/10 k_-$, $\beta = 10$, $K_+/K_- = 10$. Solutions are shown in Fig. 5.9, where the warmer is the color, the higher is the function. As Fig.5.9 shows, all solutions are almost symmetrical with respect to the $r = 15$ plane. Just like in all the previous cases, the spikes on the left are bigger (left ones are red while right ones are light orange Fig. 5.9b and 5.9c). Moreover, also Fig. 5.9a shows the characteristic symmetry, but this time one may notice that fewer free integrins are present on the square left border, for $r \simeq 20$.
Remarkably, regarding the biological system as a three state system cause

few modifications as one can see in the solutions of Fig. 5.9. First of all, introducing a finite ligand concentration cause the lowering in the ligated integrins solution Fig.5.9c with respect to the previous two state system solution; in fact, we pass from a range of $0 \div 2$ to a range of $0 \div 0.6$. This happens because integrins are no more hooking on the borders as much as in the previous two-states system. In fact, the finite ligand concentration prevent activated integrins to bound over and over as time grows. Also, activated integrins solution $n_a(r,t)$ shows no more border spikes. In fact, now, they are allowed to diffuse almost as much as free integrins. Hence, even if they activate in the borders (like in the two state system) in the three state system they can diffuse more in the activated annulus. As a result, the border spikes are not holding anymore, Fig. 5.9c.
Nevertheless, we do not remark very different behavior between the activated and ligated solutions Fig. 5.9c and Fig. 5.9b, although activated integrins show, for about $t \simeq 10$ a warmer color in the middle of the activated zone $r \simeq 15$, due again to diffusion. As a matter fo fact, as the activator u appears, about $t = 10$, activated integrins show a behavior that perfectly fit the boxcar activation function (which exhibits a maximum for $r = 15$). On the other hand, ligated integrin have to be activated first, and have to wait ligand availability to bind. That is the reason why they cannot suddenly follow the boxcar function u.
Moreover, activated integrins have higher overall value going from a range $0 \div 1.2$ while ligated integrins have a range $0 \div 0.1$. In order to see these phenomena more clearly, we can take different pictures at different times. This give a precise view of the evolution of these two states, see Fig.5.10. In Fig.5.10 we can see how the ranges are different, for instance Fig. 5.10g and Fig. 5.10h show that $n_a \simeq 10 n_l$.

5.5.3 Stationary Solutions long time limit

Another point the model must satisfy is giving the correct predictions as time tends towards infinity. In order to see that, we may try to make the simulation last longer. It should occur, of course, that as long as one waits enough time, the situation in which all three states are unchanging in time arises. This is the steady state, not to be confused with the similiar concept of chemical equilibrium, where the reaction rates in a reversible process forward and backward are equal.

As shows Fig. 5.11, the stationary states are already achieved for $t \simeq 3000$. As a matter of fact every solution tends to be completely flat for any $t \geq 3000$. Eventhough the activator is still on all integrins no matter in which state, they will spread sooner or later.

5.5.4 Recovering infinite ligand concentration

Another important aspect to be checked is the following: as soon as the ligands concentration constant c_{tot} tends towards infinity, introducing an infinite size reservoir of ligands into the system, the model should recover a behaviour similiar to the previous two-state system. Moreover, we should observe an overturning in the scales between the activated and bounded states, with respectevely less integrins in the first and more integrins in the latter.

As expected, big ligands availability does overturn the ranges of ligated and activated integrins, see Fig. 5.12b and Fig. 5.12c. This is explained by the increase in free ligands concentration. As a matter of fact, the increase of availability of free ligands increases the bounding rates so that more activated integrins are going to bind than previously. As more activated integrins are likely to bind, this lowers the number of free integrins. In the same logic, a decrease in activated integrins n_a along with an increase in ligated integrins n_l will lead to a rather small decrease in the free integrins as well as in the case $c_{\text{tot}} = 1$, Fig. 5.12a.
Another result is the evidently more convex overall surface where the step is lying, the whitish region in Fig. 5.12b and Fig. 5.12c. This is due to the diffusion term of equation (5.26). In fact, an increase in c_{tot} gives a relative increase in the diffusion in the second equation of (5.26). As there are more activated integrins in the non activated regions, then it comes straightforwardly that more integrins will bind, being greater the number of ligands. Summarizing, more integrins are present in the not activated zone thanks to diffusion and then, the number of ligated integrins grow as well, thanks to the increase in ligand disponibility, see Fig.5.12b.

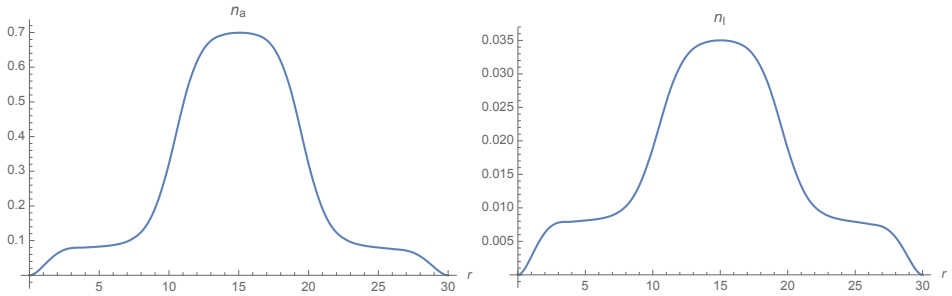

(a) $n_a(r, t = 8)$

(b) $n_l(r, t = 8)$

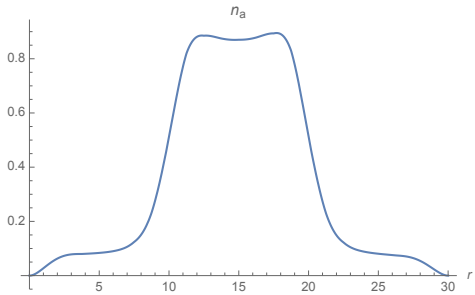

(c) $n_a(r, t = 9)$

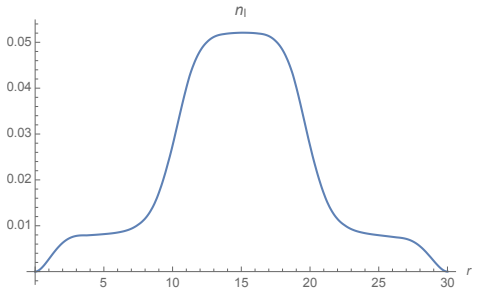

(d) $n_l(r, t = 9)$

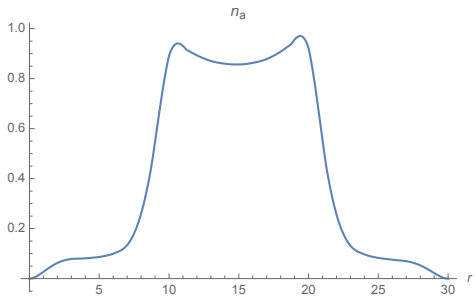

(e) $n_a(r, t = 10)$

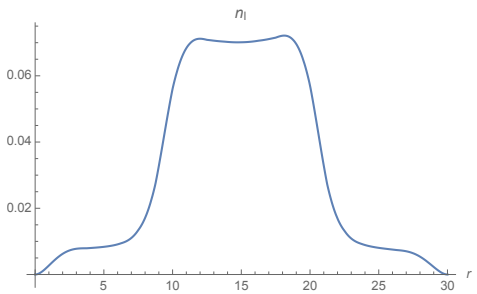

(f) $n_l(r, t = 10)$

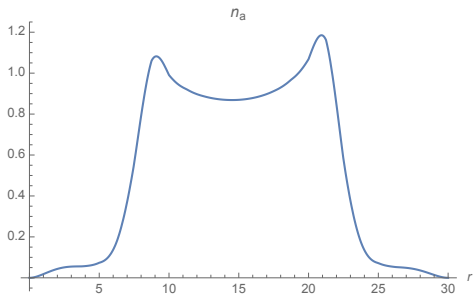

(g) $n_a(r, t = 20)$

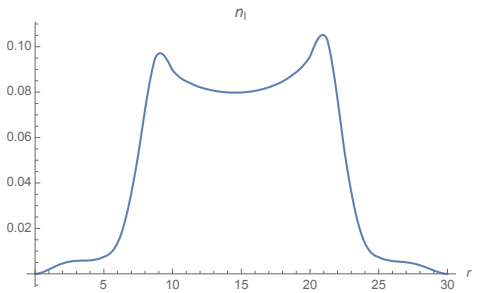

(h) $n_l(r, t = 20)$

Figure 5.10: Evolution frames of activated and bounded integrins

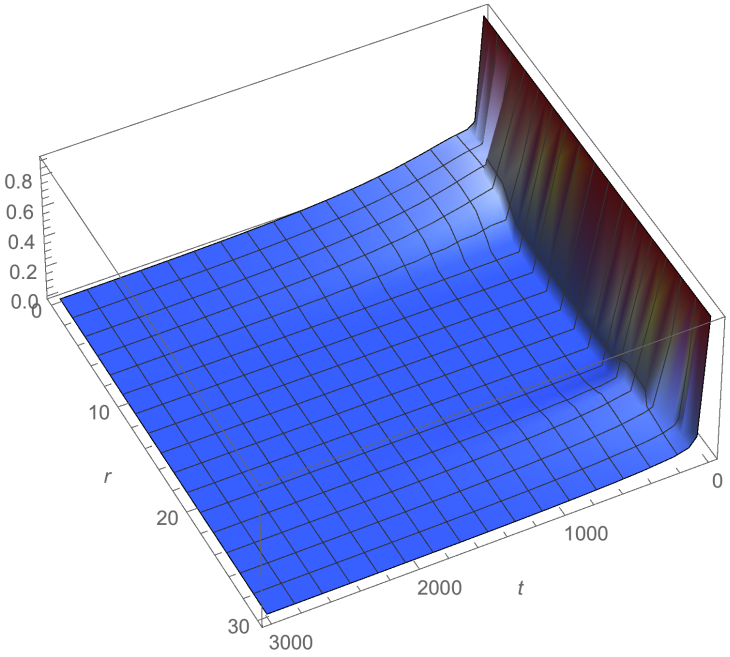

(a) $n_f(r,t)$

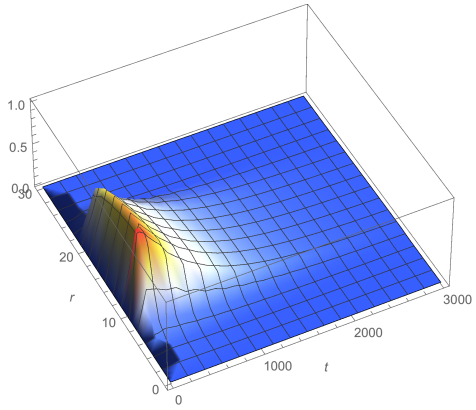

(b) $n_a(r,t)$

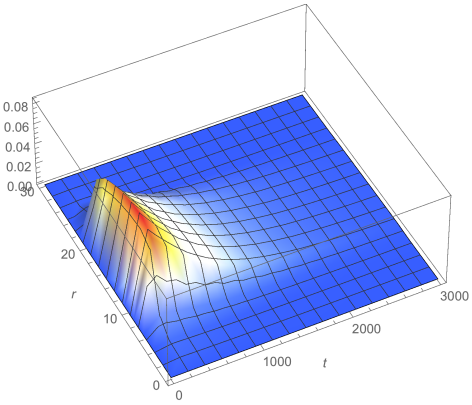

(c) $n_l(r,t)$

Figure 5.11: Solutions of the system (5.26) plotted until $t = 3000$

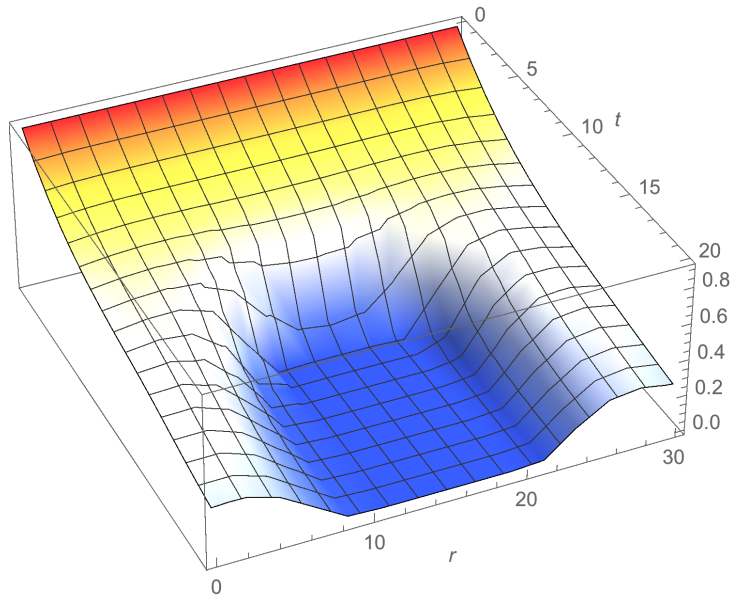

(a) n_f

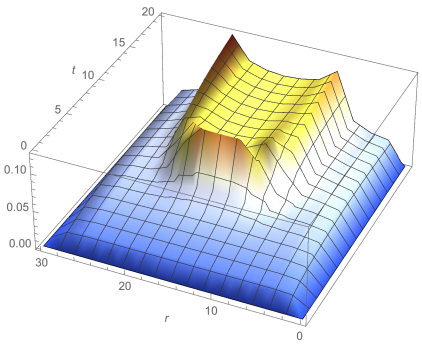

(b) n_a

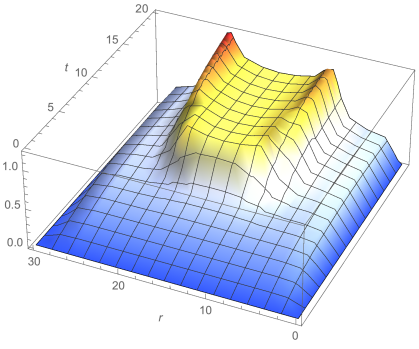

(c) n_l

Figure 5.12: Solutions of the PDE system (5.26) with a big ligands availability $c_{\text{tot}} = 100$

Chapter 6

Discussion and Conclusions

Resuming, in this work, integrin receptor activation and dynamics has been analyzed. It has been shown, that these transmembrane receptors can be idealyzed as a two-state diffusing system along with two substances, the reactor and the inihibitor which modulate activation. This reduction of the biological system down to mathematical minimal components has been made possible after an examination of the general properties of the real system. Then, retaining the major aspects, one is capable to build what is called a minimal model. This can be done on the one hand, making intense use of simplifications, so that overwhelming does not occur, and on the other hand, trying to avoid too much loss in generality. To do so, appropriate conditions were choosen that facilitate considerably calcuations without succumbing to oversimplicity. This is also done, in several cases, to keep the work amenable to analysis for the computer, which, for instance, does not seem to like step functions.
It is one of the fundamental features I learned, the capability to finely summarize the major important points of the system under consideration in order to mimic the real system. In this process, is essential the example given by the Gray-Scott model see Chapter 3, which is a tangible example and an overall similiar model to the one of the integrin receptors. The study of Gray-Scott model helped considerably in the formulation of the mathematical problem, stating the equations and the chemical reactions. Moreover, the procedures involved served as a guide throughout the whole work not only in the statement of the problem but also in the process of finding solutions and interpreting them.
Although the construction of the model is considered, by most, the most

important part, it should be remarked that it is only the first step.
Finding a solution after the problem is set is not an easy task, see Chapter 4. As a matter of fact, finding analytical solutions in these problems is a blessing. It should not surprise that in this sector, people are authentically joyous when they find an analytical solution, even for a very restricted range of the parameters involved.
In Chapter 4, we have found exact stationary solutions of pulse and kink type for the activator and the inhibitor. This was pursued with analytical methods, except for the very final plot which was done with a computer algebra program. These kinds of nontrivial patterns (pulse and kink) arise thanks to diffusion which is a feature that other existing models do not allow. As pointed out in section 4.5, the founded patterns for the inhibitor and the reactor vary in the very same range. This is a quite good feature as most of the times solutions of these equations are evaluated when the parameters varying in different ranges [9]. It is also for this specific reason that methods such asymptotic expansions are not suitable.
Finally, in Chapter 5, the behaviour and the dynamics of integrins have been investigated, resulting in some peculiar aspects. The numerical solutions for integrins were first examinated and in a second time even part of the model was modified in order to add a third state: activated but not bounded integrins. This was done together with the introduction of a finite ligand concentration. The overall properties of simulations are reasonable. Integrin motion is seen to take place mostly on the activated zone, with accumulation on the borders of the same zone. Different choosing of the rates had been there considered, and the solutions seemed to respond properly for each rate inserted. Morevover, modification of the equation of motion for integrins lead to new simulations. These simulations were find to be in agreement with different choices of the parameters.

Concluding, this work may serve as a theoretical guide for experiments probing integrins autoarrangements and organization. Also, the model can succesively be improved if found wrong on experiments. However, it is possible, thanks to its very own structure, to introduce new terms and to make minor readjustments in order to make it work in different contexts. However, this might not be always the case. In fact, even if the activation pathway postulated in this work seemed to be one of the most popular, the mechanisms of activation of these receptors are rather mysterious and

not well known. If the activation pathways is founded to be wrong we may not be able to make little readjustements to make the model work. Probably, more research is needed in this area to allow these kind of improvements.
A possible future work may be to find the various predicting behaviours of activation for different families of integrins. Moreover, attempts could be efforted in finding possible generalization of the solutions.
It is often a good task to compare solutions with other methods. In this concern, among the most common techninques we find the perturbative expansion. However, the solution evaluated with these methods cannot be compared with the ones evauated in this work. In fact, our choice of the parameters is not at all compatible with the one made in [9].
Another path one may pursue is instead seeking for some approximate analytical solutions. Among these methods the Homotopy Analysis Method (HAM) has recently become one of the most popular [8]. Ham have the great advantage that small parameters are not needed and in fact one can make vary the parameters with complete freedom.

Appendix A

Reaction Kinetics

In this appendix we illustrate how to build equation of motion from chemical reactions as found in [11]. One of the most basics enzymatic reactions involves a substrate S reacting with an enzyme E to form a complex SE which is in turn converted into a product P and the enzyme. We represent this schematically by

$$S + E \underset{\mathrm{k}_{-1}}{\overset{\mathrm{k}_1}{\rightleftarrows}} SE \xrightarrow{k_2} P + E \tag{A.1}$$

Here k_1,k_{-1} and k_2 are constant parameters associated with the rates of reaction; The double arrow symbol $\rightleftarrows$ indicates that the reaction is reversible while the single arrow $\rightarrow$ indicates that the reaction can go only on a way. The overall mechanism is a conversion of the substrate S, via the enzyme catalyst E, into a product P. In detail it says that one molecule of S combines with one molecule of E to from one of SE, which eventually produces one molecule of P and one molecule of E again. *The Law of Mass Action* states that the rate of a reaction is proportional to the product of the concentrations of the reactants in (A.1). Denoting the concentrations of reactants in (A.1) by lowercase letters

$$s = [S], \quad e = [E], \quad c = [SE], \quad p = [P], \tag{A.2}$$

where the [.] indicates concentration. Then the Law of Mass Action applied to (A.1) leads to one equation for each reactant and hence the system

of nonlinear reaction equations:

$$\begin{cases} \dfrac{ds}{dt} &= -k_1 es + k_{-1} c, \\ \dfrac{de}{dt} &= -k_1 es + (k_{-1} + k_2) \\ \dfrac{dc}{dt} &= k_1 es - (k_{-1} + k_2) c, \\ \dfrac{dp}{dt} &= k_2 c. \end{cases} \tag{A.3}$$

Bibliography

[1] Nicholas J. Anthis and Iain D. Campbell. The tail of integrin activation. *Trends Biochem Sci*, 36(4), 2011.

[2] M.R. Block, O. Destaing, C.Petropulos, E. Planus, C. Albegès-Rizo, and B. Fourcade. Integrin mediated adhesion as self-sustained waves of enzymatic activation. *Phys. Rev. E*, 92(4), October 2015.

[3] Bell GI. Models for the specific adhesion of cells to cells. *Science*, 200(4342):618–627, May 1978.

[4] B. P Ingalls. *Mathematical Modeling in Systems Bi- ology: An Introduction*. The MIT Press, Cambridge, 2013.

[5] W.C. Troy J.K. Hale, L.A. Peletier. Exact homoclinic and heteroclinic solutions of the gray-scott model for autocatalysis. *Siam J. Appl. Math*, 61(1):102–130, 2000.

[6] K. Kelly. *Out of Control: The New Biology of Machines, Social Systems, & the Economic World*. New York: Basic Books., 1995.

[7] Y. Lazebnik. Can a biologist fix a radio?—or, what i learned while studying apoptosis. *Cancer Cell*, 2:179–182, (2002).

[8] S.J. Liao. *The proposed homotopy analysis technique for the solution of nonlinear problems*. PhD thesis, Shanghai Jiao Tong University, 1992.

[9] C. B. Muratov and Osipov. Static spike autosolitons in the gray-scott model. *J. Phys. A: Math Gen*, 33:8893–8916, 2000.

[10] J. D. Murray. *Mathematical Biology II: Spatial Models and Biomedical Applications*, volume II. New York: Springer., 3rd edition, 2003.

[11] J.D. Murray. *Mathematical Biology I. An Introduction*, volume 17. Springer, third edition, 2002.

[12] D. Noble. Modeling the heart. *Physiology*, 19:191–197, 2004.

[13] S.K. Scott P. Gray. Autocatalytic reactions in the isothermal continuous stirred tank reactor: Isolas and other forms of multistability. *Chem Engrg. Sci.*, 38:29–43, 1983.

[14] J. Rinzel. Discussion: Electrical excitability of cells, theory and experiment: Review of the hodgkin-huxley foundation and an update. *Bulletin of Mathematical Biology*, 52:5–23, 1990.